eNeuro

Research Article: New Research | Neuronal Excitability

Corticotropin releasing factor receptor-1 neurons in the lateral amygdala display selective sensitivity to acute and chronic ethanol exposure

https://doi.org/10.1523/ENEURO.0420-19.2020

Cite as: eNeuro 2020; 10.1523/ENEURO.0420-19.2020

Received: 10 October 2019
Revised: 15 January 2020
Accepted: 28 January 2020

1. Title: Corticotropin releasing factor receptor-1 neurons in the lateral amygdala display selective sensitivity to acute and chronic ethanol exposure

2. Abbreviated Title: Ethanol sensitivity and phenotype of LA CRF1 neurons

3. Authors: AE Agoglia[1,2], M Zhu[3], R Ying[1,2], H Sidhu[4], LA Natividad[4], SA Wolfe[4], MW Buczynski[5], C Contet[4], LH Parsons[4], M Roberto[4], MA Herman[1,2*]

[1]Department of Pharmacology, [2]Bowles Center for Alcohol Studies, [3]Neuroscience Curriculum, University of North Carolina at Chapel Hill, School of Medicine, Chapel Hill, NC 27599; [4]Department of Neuroscience, The Scripps Research Institute La Jolla, CA 92037; [5]School of Neuroscience, Virginia Polytechnic Institute and State University, Blacksburg, VA 24061

4. Contributions: MAH, RM, LHP, CC designed research; MH, SAW performed research; AEA, MZ, RY, LAN, SAW analyzed data; AEA, MZ, RY, MH, LAN, SAW, wrote paper.

5. Correspondence should be addressed to:
Melissa Herman, Ph.D.
104 Manning Dr. CB7178
1027 Thurston Bowles Bldg. Chapel Hill, NC 27599
(919) 445-3855 melissa_herman@unc.edu

6. Number of figures: 10

7. Number of tables: 0

8. Number of multimedia: 0

9. Number of words- Abstract: 246

10. Number of words- significance statement:

11. Number of words- Introduction: 655

12. Number of words- Discussion: 1552

13. Acknowledgements: We thank Ilham Polis for technical assistance with the microdialysis experiments and Elizabeth Crofton for manuscript review.

14. Conflict of interest: Authors report no conflict of interest.

15. Funding: This work was supported by the Bowles Center for Alcohol Studies, NIH grants T32AA007573 (AEA), T32NS007431 (MZ), AA023002 (MH), AA011605 (MH), AA015566 (MR), AA021491 (MR), AA006420 (MR,CC), T32AA007456 (SAW), AA026685 (CC), AA024952 (HS).

ABSTRACT

The lateral amygdala (LA) serves as the point of entry for sensory information within the amygdala complex, a structure that plays a critical role in emotional processes and has been implicated in alcohol use disorders. Within the amygdala, the corticotropin-releasing factor (CRF) system has been shown to mediate some of the effects of both stress and ethanol, but the effects of ethanol on specific CRF1 receptor circuits in the amygdala have not been fully established. We used male CRF1:GFP reporter mice to characterize CRF1-expressing (CRF1+) and non-expressing (CRF1-) LA neurons and investigate the effects of acute and chronic ethanol exposure on these populations. The CRF1+ population was found to be comprised predominantly of glutamatergic projection neurons with a minority subpopulation of interneurons. CRF1+ neurons exhibited a tonic conductance that was insensitive to acute ethanol. CRF1- neurons did not display a basal tonic conductance, but application of acute ethanol induced a δ $GABA_A$ receptor subunit-dependent tonic conductance and enhanced phasic GABA release onto these cells. Chronic ethanol increased CRF1+ neuronal excitability but did not significantly alter phasic or tonic GABA signaling in either CRF1+ or CRF1- cells. Chronic ethanol and withdrawal also did not alter basal extracellular GABA or glutamate transmitter levels in the LA/BLA and did not alter sensitivity of GABA or glutamate to acute ethanol-induced increases in transmitter release. Together, these results provide the first characterization of the CRF1+ population of LA neurons and suggest mechanisms for differential acute ethanol sensitivity within this region.

SIGNIFICANCE STATEMENT

The corticotropin releasing factor (CRF) system is a critical component of the stress network and has been implicated in psychiatric disorders including addiction, anxiety, and depression. The present study examines CRF receptor-1 (CRF1) lateral amygdala (LA) neurons and reports differential inhibitory control and acute ethanol effects of CRF1 LA neurons as compared to the unlabeled (CRF1-) population. An improved understanding of CRF1 amygdala circuitry and the selective sensitivity of that circuitry to ethanol represents an important step in identifying brain region-specific neuroadaptations that occur with ethanol exposure. The present findings also have broad implications, including potential relevance to the role of CRF1 circuitry in other contexts that may provide insight into other disorders involving amygdala dysfunction, including anxiety and depression.

INTRODUCTION

The amygdala complex has been implicated in a number of important functions, notably emotional processing of internal and external sensory stimuli and the coordination of relevant behavioral output (Pitkanen et al., 1997). Amygdala dysfunction is implicated in anxiety (Tye et al., 2011) and alcohol abuse disorders (Koob et al., 1998). The lateral amygdala (LA) serves as the entry point for sensory information and sends excitatory projections to other amygdala nuclei, including the central (CeA) and basolateral amygdala (BLA), to facilitate stimuli processing (Sah et al., 2003; Agoglia and Herman, 2018). The LA is required for the acquisition and expression of fear learning and memory (Sears et al., 2014), and plays a crucial role in the development of anxiety-like behaviors (Rodrigues et al., 2004). Similar mechanisms may be involved in the dysregulated amygdalar activity seen in alcohol dependence (McCool et al., 2010), but the diversity of cell types within the LA complicates the interpretation of ethanol effects.

GABAergic neurotransmission is sensitive to acute and chronic ethanol exposure, and $GABA_A$ receptor activity is involved in ethanol tolerance and dependence. (Eckardt et al., 1998; Grobin et al., 1998; Weiner and Valenzuela, 2006). Both phasic (immediate, short-term inhibition) and tonic (persistent inhibition) GABAergic transmission within the CeA is sensitive to acute and chronic ethanol in a cell type-specific manner (Herman et al., 2013; Herman et al., 2016). The functional characteristics of $GABA_A$ receptors are determined by their subunit composition; receptors containing the α4, α6, and/or δ subunit are expressed extrasynaptically and mediate tonic conductance (Semyanov et al., 2004). These receptors also display an increased sensitivity to ethanol (Wallner et al., 2003; Wei et al., 2004), and may be a primary target for ethanol in the brain (Wallner et al., 2003; Mody et al., 2007), although the direct action of ethanol on tonic $GABA_A$ receptors remains controversial (Borghese and Harris, 2007; Baur et al., 2009). Tonic inhibition has been described in principal cells and local interneurons in the LA, but the receptor composition mediating this tonic conductance in LA neurons is unclear (Marowsky et al., 2012).

Corticotropin releasing factor (CRF) and the CRF receptor-1 (CRF1) are expressed throughout the amygdala (Van Pett et al., 2000; Calakos et al., 2017) and have been implicated in neuroplastic changes related to fear (Hubbard et al., 2007), anxiety (Overstreet et al., 2004; Rainnie et al., 2004) and alcohol exposure (Nie et al., 2004; Roberto et al., 2010; Herman et al., 2013; Lovinger and Roberto, 2013). Notably, activation of CRF1 receptors increases the excitability of BLA neurons to sensory input (Ugolini et al., 2008) and administration of CRF into the BLA increases activation of calcium/calmodulin dependent protein kinase II (CaMKII)-containing projection neurons

(Rostkowski et al., 2013). Despite the expression of CRF and CRF1 in the LA and the relevance of the CRF system to the consequences of ethanol exposure, the specific effects of ethanol on the LA CRF1 neuronal population have not been characterized.

Previous work utilizing a transgenic mouse line expressing green fluorescent protein (GFP) under the *Crhr1* promoter (Justice et al., 2008) found that CRF1+ and CRF1- neurons within the CeA exhibit distinct inhibitory characteristics and differential sensitivity to acute and chronic ethanol (Herman et al., 2013; Herman et al., 2016). The CRF1-containing neuronal population within the LA has not been previously characterized, and could be an important determinant of LA activity and output as well as a site of action for drugs of abuse such as ethanol. The current study utilizes the same CRF1:GFP mice to selectively target and characterize CRF1 neurons in the LA, not to probe the effect of CRF1 activation, which will be the subject of future studies. Here, we combine electrophysiology, immunohistochemistry and microdialysis to (1) characterize the phenotype of CRF1+ and CRF1- neurons of the LA, (2) investigate phasic and tonic inhibitory transmission in LA CRF1+ and CRF1- cells, and (3) determine the effects of acute and chronic ethanol exposure on inhibitory control within the LA.

MATERIALS AND METHODS

Animals

Experiments were performed in 59 adult (3-6 months, 19-30 g) male transgenic CRF1:GFP mice that express green fluorescent protein (GFP) under the *Crhr1* promoter, as previously described (Justice et al., 2008). Mice were bred and group

housed in a temperature and humidity controlled 12hr light/dark facility with *ad libitum* access to food and water. All experiments were performed in tissue collected from mice between Zeitgeber 2-7. All procedures were approved by the Scripps Research Institute and the University of North Carolina Chapel Hill Institutional Animal Care and Use Committees.

Electrophysiological recording

Coronal sections (300 μm) were prepared with a Leica VT1000S (Leica Microsystems) from brains that were rapidly extracted from mice after brief anesthesia (5% isoflurane) and placed in ice-cold sucrose solution containing (in mM): sucrose 206.0; KCl 2.5; $CaCl_2$ 0.5; $MgCl_2$ 7.0; NaH_2PO_4 1.2; $NaHCO_3$ 26; glucose 5.0; HEPES 5. After sectioning, slices were incubated in an oxygenated (95% O_2/5% CO_2) artificial cerebrospinal fluid (aCSF) solution containing (in mM): NaCl 130, KCl 3.5, NaH2PO4 1.25, MgSO4 1.5, CaCl2 2, NaHCO3 24, glucose 10 for 30 min at 37 °C, followed by 30 min equilibration at room temperature (21–22 °C). Recordings were made with patch pipettes (3-6 MΩ; Warner Instruments) filled with an intracellular solution containing (in mM): KCl 145; EGTA 5; $MgCl_2$ 5; HEPES 10; Na-ATP 2; Na-GTP 0.2, coupled to a Multiclamp 700B amplifier (Molecular Devices), acquired at 10kHz, low-pass filtered at 2-5 kHz, digitized at 20kHz (Digidata 1440A; Molecular Devices), and stored on a computer using pClamp 10 software (Axon Instruments). Series resistance was typically <15 MΩ and was continuously monitored with a hyperpolarizing 10 mV pulse; neurons with series resistance greater than 15 MΩ or >20% change in resistance during recording were excluded from final analysis. Lateral amygdala (LA) neurons containing the CRF1 receptor were identified by GFP expression and differentiated from unlabeled

(GFP-) neurons using fluorescent optics and brief (<2 s) episcopic illumination in slices from CRF1:GFP reporter mice. Electrophysiological properties of cells were determined by pClamp 10 Clampex software online during voltage-clamp recording using a 10 mV pulse delivered after breaking into the cell. Drugs were applied either by bath or Y-tube application for local perfusion. Recordings (V_{hold}= -60mV) were performed in the presence of the glutamate receptor blockers 6,7-dinitroquinoxaline-2,3-dione (DNQX, 20 μM) and DL-2-amino-5-phosphonovalerate (AP-5, 50 μM) and the $GABA_B$ receptor antagonist CGP55845A (1 μM). All recordings were conducted at room temperature and all solutions (bath and y-tube) were prepared and maintained at room temperature.

Drugs and Chemicals

DNQX (6,7-dinitroquinoxaline-2,3-dione, 10 μM), AP-5 (DL-2-amino-5-phosphonovalerate, 50 μM) and CGP 55845A (1 μM) were purchased from Tocris Bioscience. SR-95531 (gabazine, GBZ; 100 μM), picrotoxin (PTX 100 μM), and 4,5,6,7-tetrahydroisoxazolo[5,4-c]pyridin-3-ol (THIP, 1-10 μM) were purchased from Sigma.

Immunohistochemistry

Mice (n = 4) were anesthetized with isoflurane and perfused with cold phosphate buffered saline (PBS) followed by 4% paraformaldehyde (PFA). Brains were dissected and immersion fixed in PFA for 24 hours at 4°C, cryoprotected in sterile 30% sucrose in PBS for 24-48 hours at 4°C or until brains sank, flash frozen in pre-chilled isopentane on dry ice and stored at -80°C. Free floating 35 μm brain sections were obtained using a cryostat and kept at 4°C in PBS containing 0.01% sodium azide.

171 Sections were washed in PBS for 10 minutes at room temperature (RT) with
172 gentle agitation and then blocked for 1 hour at RT in blocking solution [0.3% triton X-
173 100, 1mg/ml bovine serum albumin (BSA) and 5% normal goat serum (NGS)]. Primary
174 antibody was incubated at 4^0C overnight with gentle agitation in 0.5% tween-20 and 5%

175 NGS. The following primary antibodies were used: chicken anti-GFP (Abcam, ab13970,
176 RRID:AB 300798; 1:2000), rabbit anti-α1 and rabbit anti-δ $GABA_A$ receptor subunit
177 (812-GA1N, 868A-GDN;1:100; PhosphoSolutions), mouse anti-parvalbumin (Swant,
178 235, RRID:AB 10000343; 1:1000), mouse anti-calretinin (Swant, 6B3, RRID:AB
179 10000320; 1:500) and mouse anti-calbindin (Swant, 300, RRID:AB 10000347; 1:2000).
180 Antibodies against native mouse protein were validated by the manufacturer with tissue
181 from knockout mice, with the exception of anti-δ $GABA_A$. Next, sections were triple
182 washed in PBS for 10 minutes at RT with gentle agitation followed by a 1 hour
183 secondary antibody incubation in PBS (in the dark). The following secondary antibodies
184 were used: Alexa Fluor 488 goat anti-chicken (Thermo Fisher Scientific, A-11039,
185 RRID:AB 142924), Cy-3 donkey anti-rabbit (Jackson Immuno, 711-165-152, RRID:AB
186 2307443) and Alexa Fluor 568 goat anti-mouse (Thermo Fisher Scientific, A-11004,
187 RRID:AB 141371). Sections were then washed (10 minutes, RT, 3 times) and mounted
188 in Vectashield (Vector labs, H1500, RRID:AB 2336788).

189 Sections were imaged on a Zeiss LSM 780 laser scanning confocal microscope
190 (10x objective, tile scanning of LA). All microscope settings were kept the same within
191 experiments during image acquisition. Analyst was blind to the identity of the red
192 fluorescent signal when performing cell counts, and analysis was performed manually in

an unbiased manner at four anterior-posterior levels (equidistant sections located -1.00 through -1.70 mm from bregma). Data are presented as mean ± standard error.

In situ hybridization

Mice (n=3) were perfused with ice cold PBS/Z-fix (Fisher Scientific, NC9378601) after anesthesia with isoflurane. Following perfusion, brains were dissected and immersion fixed for 24 hours in Z-fix at 4°C, cryoprotected in 30% sucrose in PBS for 24 hours at 4°C, and flash frozen in isopentane on dry ice. Brains were preliminarily stored at -80°C until they were sliced on a cryostat in 20 µm thick sections, mounted on SuperFrost Plus slides (Fisher Scientific, 1255015), and stored at -80°C.

Using an RNAscope fluorescent multiplex kit (ACD, 320850) *in situ* hybridization was performed for *Crhr1*, *Gfp* and *Slc17a7*. Target retrieval pretreatment as outlined in the manual provided by RNAscope (ACD, doc. no. 320535) was performed by first briefly washing prepared slides in PBS. Next slides were submerged in prewarmed target retrieval buffer (ACD, cat. no. 322000) kept at a constant temperature between 95–98°C for 10 min. Slides were then removed and immediately rinsed in distilled water twice, and then dehydrated with 100% ethanol. After dehydrations, slices were demarcated with a hydrophobic barrier pen (ACD, cat. no. 310018) and digested with Protease IV for 20 min at 40°C in a hybridization oven. Next, the RNAscope Fluorescent Multiplex Reagent Kit User Manual (ACD, doc.no. 320293) was followed entirely. Lastly, slides were mounted with Vectashield with DAPI (Fisher Scientific, NC9029229). The probes used from ACD Biotechne were *Crhr1* (418011-C2, probe target region 207-

813), *Slc17a7* (416631-C1, probe target region 464-1415), eGFP (400281, probe target region 628-1352) and negative control (320751).

Slides were imaged on a Zeiss LSM 780 laser scanning confocal microscope (40X oil immersion, 1024x1024, of LA at approximately bregma -1.46mm, 5-µm z-stacks). All microscope settings were kept the same within experiments during image acquisition. Background was subtracted from images based on the negative control for each probe, and signal intensity present in DAPI labeled nuclei after background subtracted denoted positive cells. To perform quantification, ImageJ was used to manually count DAPI labeled nuclei expressing fluorescently labeled probes in the region of interest (ROI). Next, the percentage of nuclei positive for one or both probes and the percent of signal co-localization were calculated. The percent of *Crhr1*+ nuclei expressing a marker of interest was determined by dividing the number of co-labeled nuclei by the total number of *Crhr1*+ nuclei. Quantification was performed on 3-4 images (~bregma -1.46mm) from each mouse in an unbiased manner as probe fluorescence was quantified blindly. Brightness/contrast and pixel dilation are the same for all representative images.

Chronic intermittent ethanol vapor inhalation

Mice were placed in ethanol inhalation chambers (La Jolla Alcohol Research) and exposed to chronic intermittent ethanol (CIE) vapor (16h) followed by air (8h) daily for 4 consecutive days/week for a period of 4–5 weeks (Herman et al., 2016). Before each vapor exposure, CIE mice were injected with a solution of ethanol (1.5g/kg) and pyrazole (1mmol/kg, i.p.), an alcohol dehydrogenase inhibitor, to initiate intoxication and maintain constant blood alcohol levels (BALs). Control mice were exposed to room air

and received an injection of pyrazole (1 mmol/kg, i.p.) at the onset of each ethanol vapor exposure. Ethanol drip rate and air flow were adjusted so as to yield BALs averaging 100–250 mg/dl. BALs were measured throughout exposure using an Analox GM7 analyzer. Average BALs for the CIE mice included in electrophysiological recordings were 174.6 ± 15.5 mg/dL. Average BALs for CIE mice in microdialysis experiments were 162.7 ± 16.5 mg/dL. Terminal BALs were also determined at the time of death when mice were euthanized immediately after their last ethanol vapor exposure (CIE mice). Another group of mice underwent 3–7 days of withdrawal after their last vapor exposure before being euthanized (CIE-WD mice).

Microdialysis

Mice (n = 11) were unilaterally implanted with custom fabricated microdialysis probes (0.5 mm regenerated cellulose) aimed at the LA (from bregma: anteroposterior: -1.5 mm; mediolateral: +/- 2.9 mm; dorsoventral: -4.1 mm from dura). However, as some penetrance into BLA is possible, microdialysis results are described throughout as LA/BLA. Mice were perfused with aCSF at 0.2 µl/min and allowed to recover overnight, as previously described (Pavon et al., 2018a; Pavon et al., 2018b). The following morning, the flow rate was increased to 0.6 µl/min and allowed to equilibrate for 60 min prior to collection. Dialysate samples were collected at 15 min intervals during a 1.5 h baseline period. Ethanol (1 M) was added to the aCSF perfusate solution for reverse dialysis through the probe, and samples were collected for an additional 1.5 h during the local ethanol exposure period. This dose of ethanol was chosen for consistency with prior experiments utilizing reverse dialysis in rodents, where 1 M was found to induce

maximal changes in extracellular GABA and glutamate levels (Roberto et al., 2004a; Roberto et al., 2004b).

Quantification of neurotransmitters was performed using triple liquid chromatography quadrupole mass spectrometry (LC-MS/MS) methods as previously described (Song et al., 2012; Buczynski et al., 2016). Briefly, microdialysate samples (5 µL) were derivatized with 100 mM borate (5 µL), 2% benzoyl chloride (2 µL, in acetonitrile) and 1% formic acid (2 µL) and subsequently spiked with benzoylated $^{13}C_6$-labeled internal standards (5 µl, in 98% v/v of ACN, 1% formic acid, and 1% H_2O). Samples (10 µl, 4°C) were separated by high performance liquid chromatography and analyzed by positive-ion mode tandem quadrupole mass spectrometry (Agilent 6460 QQQ) using multiple-reaction monitoring. The following neurotransmitters were quantified using the standard isotope dilution method (precursor→product): the amino acids aspartate (238→105), GABA (208→105), glutamate (252→105), glutamine (251→105), glycine (180→105), serine (210→105), and taurine (230→105). Baseline concentrations were expressed as an absolute value (nM), while changes produced by ethanol reverse dialysis were expressed as relative values (% of baseline) over time.

Statistical Analysis

Membrane characteristics and excitability were compared between groups using a two-tailed t-test or a one-way ANOVA, where appropriate. Frequency, amplitude and decay of spontaneous inhibitory postsynaptic currents (sIPSCs) were analyzed and visually confirmed using a semi-automated threshold based mini detection software (Mini Analysis, Synaptosoft Inc.). sIPSC characteristics were determined from baseline

and experimental drug conditions containing a minimum of 60 events (time period of analysis varied as a product of individual event frequency). All detected events were used for analysis and superimposed events were eliminated. Tonic conductance was determined using Clampfit 10.2 (Molecular Devices) and a previously-described method (Belelli et al., 2009) in which the mean holding current (i.e., the current required to maintain the -60 mV membrane potential) was obtained by a Gaussian fit to an all-points histogram over a 5 sec interval. The all-points histogram was constrained to eliminate the contribution of sIPSCs to the holding current. Drug responses were quantified as the difference in holding current between baseline and experimental conditions. Events were analyzed for independent significance using a one-sample t-test and compared using a two-tailed t-test for independent samples, a paired two-tailed t-test for comparisons made within the same recording, and a one-way ANOVA for comparisons made between 3 or more groups. In the microdialysis experiments, average baseline concentrations of glutamate and GABA were compared in CIE-WD versus AIR controls using two-tailed t-tests. To examine the effects of acute ethanol administration on LA/BLA dialysate, two-way repeated measures RM-ANOVA (exposure condition X time) was used to compare air to CIE-WD mice before and after reverse dialysis of ethanol. All statistical analyses were performed using Prism 5.02 (GraphPad, San Diego, CA). Data are presented as mean ± standard error. In all cases, $p<0.05$ was the criterion for statistical significance.

RESULTS

Phenotype of CRF1+ LA neurons

To validate the fidelity of the CRF1:GFP expression in the LA, we used the RNAscope assay (n = 11 images from 3 mice) to examine co-localization of *Crhr1*, the transcript for CRF1, and *Gfp,* the transcript for green fluorescent protein (**Figure 1A**). The number of positive nuclei in the region of interest (ROI) was consistent between groups (**Figure 1B**). Approximately 74% of *Crhr1*+ neurons co-express *Gfp* and 84% of *Gfp*+ neurons co-express *Crhr1* (**Figure 1C**), indicating substantial penetrance and fidelity, respectively. To identify the phenotype of CRF1+ neurons in the LA, we performed *in situ* hybridization in brain sections from CRF1:GFP mice (n = 10 images from 3 mice) to examine co-localization of *Crhr1* and *Slc17a7*, the transcript for the vesicular glutamate transporter VGLUT1. Consistent with GFP expression and the established glutamatergic makeup of the BLA, *Crhr1* and *Slc17a7* were similarly expressed in the LA (**Figure 1D-F**). The number of positive nuclei counted in the ROI was not significantly different between *Slc17a7*+ and *Crhr1*+ (**Figure 1G**). Approximately 60% of *Slc17a7*+ neurons co-express *Crhr1* and ~80% of *Crhr1*+ neurons co-express *Slc17a7* (**Figure 1H**). These data suggest that *Crhr1*+ neurons make up a subpopulation of LA glutamatergic cells and that the majority of *Crhr1*+ LA neurons are glutamatergic.

The LA is composed of glutamatergic projection neurons as well as local GABAergic interneurons (Sosulina et al., 2006). The results of the *in situ* experiments indicated that a subpopulation of the CRF1+ neurons of the LA do not express *Slc17a7*, suggesting that these neurons are not glutamatergic but may express calcium binding proteins (CBPs) associated with GABAergic interneurons. Work by Calakos et al. (2017) reported that the majority of parvalbumin (PV)-containing neurons in the BLA also

expressed CRF1, but the expression of CBPs in CRF1+ neurons of the LA is unknown. We examined PV and GFP colocalization in the LA of CRF1:GFP mice (n = 16 sections from 4 mice) as well as calbindin (CB) and calretinin (CR). For the purpose of clarity, we refer to GFP+ and GFP- neurons throughout as CRF1+ and CRF1-, respectively. We observed expression of CB, CR, and PV interspersed with GFP in the LA (**Figure 2A, 2B, and 2C**), but there were more CRF1+ cells than CBP-containing cells (**Figure 2D**). Consistent with Calakos et al., we observed that a substantial percentage (~80%) of CBP+ cells also expressed GFP (**Figure 2E**), suggesting that the majority of LA neurons that express CBPs also contain CRF1. However, the percentage of CRF1+ neurons that contain CBPs was much lower (<20%, **Figure 2F**), suggesting that the majority of CRF1+ neurons are likely not interneurons that express these calcium binding proteins. Together, the results of the *in situ* and immunohistochemistry experiments identify the CRF1+ neurons of the LA as a mostly (~80%) glutamatergic population with a smaller (~20%) population of neurons that express CBPs (potentially GABAergic interneurons).

Membrane Properties and Excitability

LA neurons were identified and targeted for electrophysiological recording based on GFP expression. CRF1+ neurons (n = 28 cells from 14 mice) possessed a significantly smaller membrane capacitance [t (54) = 2.96, p = 0.0046 by unpaired t-test, 21.84 ± 7.39 pF effect size with 95% confidence interval -36.65 to -7.02], increased membrane resistance [t (30) =2.34, p = 0.0260 by unpaired t-test, 99.46 ± 42.48 mV effect size with 95% confidence interval of -186.2 to -12.71], lower time constant [t (54) = 3.08, p = 0.0033 by unpaired t-test, 226 ± 73.56 ms effect size with 95% confidence

interval of -373.6 to -78.69] and higher resting membrane potential [*t* (54) = 3.95, *p* = 0.0002 by unpaired t-test, 9.114 ± 2.31 mV effect size with 95% confidence interval of 4.49 to 13.74) as compared to CRF1- neurons (n = 28 cells from 15 mice; **Figure 3A**). Whole-cell current-clamp recordings and a step protocol consisting of hyperpolarizing (-60 pA) to depolarizing (100 pA, **Figure 3B and 3C**) current injections were used to examine the spiking properties of CRF1+ and CRF1- LA neurons. The large majority (90%) of CRF1+ neurons exhibited spike accommodation (**Figure 3B, bottom**) whereas CRF1- neurons were more variable (52% accommodating, **Figure 3C, bottom**). We observed no significant differences in rheobase between CRF1+ (37.52 ± 10.11 pA) and CRF1- neurons (55.94 ± 8.90 pA; **Figure 3D**, **left**), however we did observe a significantly lower threshold to fire in CRF1- neurons (-48.64 ± 1.25 pA) versus CRF1+ neurons [-44.61 ± 0.78 pA; *t* (40) =2.73, *p* = 0.0093, effect size 4.03 ± 1.48 pA with 95% confidence interval of -7.01 to -1.048; **Figure 3D**, **right**]. In addition, we found no differences in action potentials elicited by ascending current injection between CRF1+ and CRF1- neurons (**Figure 3E**).

Phasic and Tonic Inhibitory Transmission

Whole-cell voltage clamp recordings of spontaneous inhibitory postsynaptic currents (sIPSCs) were performed to assess baseline phasic inhibitory transmission. CRF1+ neurons had a significantly higher average baseline sIPSC frequency (9.0 ± 1.8 Hz; n = 7 cells from 6 mice; **Figure 4A and B**) as compared to CRF1- neurons [3.3 ± 0.6 Hz; *t*(14) = 3.30, *p*= 0.0053 by unpaired t-test, 5.71 ± 1.73 Hz effect size with 95% confidence interval of 2.00 to 9.42; n = 9 cells from 5 mice **Figure 4A and B**) and no difference in sIPSC amplitude (51.01 ± 5.0 and 54.7 ± 5.7 pA, p = 0.64; **Figure 4A and**

372 **B**), decay (2.77 ±0.08 and 3.60 ±0.5 ms, p = 0.17; **Figure 4A and B**) or rise time (1.61 ±
373 0.12 and 1.58 ± 0.16 ms, p = 0.88) between CRF1+ and CRF1- LA neurons,
374 respectively.

375 We assessed tonic conductance in CRF1+ (n = 7 cells from 5 mice) and CRF1-
376 (n = 9 cells from 5 mice) LA neurons using whole-cell voltage clamp recordings. Basal
377 holding current was -28.32 ± 20.67 pA in CRF1+ neurons and -17.19 ± 14.65 pA in
378 CRF1- neurons. A $GABA_A$ receptor-mediated tonic current was defined as the
379 difference in holding current (i.e., the current required to maintain the neuron at -60mV)
380 before and after application of a $GABA_A$ receptor antagonist. Focal application of the
381 $GABA_A$ receptor antagonist gabazine (GBZ, 100 μM) produced a significant reduction in
382 holding current in CRF1+ neurons (9.2 ± 1.8 pA, n = 7; **Figure 4C left trace** and **Figure**
383 **4D;** $t(14) = 5.56$, $p = 0.002$ by one sample t-test, 9.45 ± 1.70 pA effect size with 95%
384 confidence interval of 5.81 to 13.09) and a reduction in the amplitude of the holding
385 current or root mean square (RMS) noise (6.4 ± 0.7 to 5.4 ± 0.4 pA; **Figure 4E, left**
386 **panel;** $t(6) = 2.93$, $p = 0.0264$ by paired t-test, 1.06 ± 0.364 pA effect size with 95%
387 confidence interval of 0.17 to 1.94). In CRF1- neurons, focal application of gabazine
388 (GBZ, 100 μM) produced no change in holding current (-0.3 ± 0.6 pA, n = 9; **Figure 4C**
389 **right trace** and **Figure 4D;** $p = 0.6568$ by one sample t-test) and a reduction in RMS
390 noise of a much smaller magnitude [5.6 ± 0.3 to 5.1 ± 0.3 pA; **Figure 4E, right panel;**
391 $t(8) = 5.24$, $p = 0.0008$ by paired t-test, 0.51 ± 0.10 pA effect size with 95% confidence
392 interval of 0.29 to 0.74). The reduction in holding current was significantly greater in
393 CRF1+ neurons as compared to CRF1- neurons (**Figure 4D** $t(14) = 5.56$, $p = 0.0001$ by

unpaired t-test, 9.45 ± 1.70 pA effect size with 95% confidence interval of 5.81 to 13.09).

Expression of $GABA_A$ receptor subunits

The phasic and tonic conductance of $GABA_A$ receptors is dependent upon specific subunit configurations and/or expression. We performed double-label immunohistochemical studies examining α1 and δ $GABA_A$ receptor subunit expression in CRF1+ and CRF1- neurons in the LA (n = 12 sections from 4 mice). The LA contains a significant number of CRF1+ cells, in contrast with sparse GFP expression in the BLA (**Figure 5A and 5D**). The α1 $GABA_A$ receptor subunit has dense expression in the LA (**Figure 5B**) and displays co-localization with GFP (**Figure 5C**), indicating expression in the majority of CRF1+ neurons. In contrast, δ $GABA_A$ receptor subunit expression was greater in the body of the BLA than in the LA (**Figure 5E**) and displays minimal co-localization with GFP (**Figure 5F**), indicating little to no expression in CRF1+ neurons in the LA.

The δ subunit is associated with tonic conductance in a number of brain areas including the hippocampus, cerebellum, cortex, and amygdala (Saxena and Macdonald, 1996; Stell et al., 2003; Krook-Magnuson and Huntsman, 2005). Thus, we examined the functional contribution of δ subunit-containing $GABA_A$ receptors in the LA using the δ subunit-preferring agonist gaboxadol (THIP, 5 μM). Focal application of THIP produced a modest increase in holding current in CRF1+ neurons [7.5 ± 2.4 pA; n = 6 cells from 6 mice; $t(5) = 3.12$, $p = 0.0262$ by one sample t-test, **Figure 6A**, left trace and **Figure 6B**] and CRF1- neurons [25.9 ± 3.8 pA; n = 14 cells from 10 mice, $t(13) = 6.82$, $p < 0.001$ by

one sample t-test; **Figure 6A** right trace and **Figure 6B**]**.** This increase was significantly greater in CRF1- neurons as compared with CRF1+ neurons [t (18) = 3.03, *p = 0.0072 by unpaired t-test, 18.44 ± 6.09 pA effect size with 95% confidence interval of -31.24 to -5.65]. Consistent with the observed effects on holding current, focal application of THIP onto CRF1+ neurons resulted in no change in the amplitude of the holding current or RMS noise (6.6 ± 0.9 to 6.5 ± 0.7 pA; **Figure 6C, left panel** p = .9183 by paired t-test) but significantly increased RMS noise in CRF1- neurons (6.4 ± 0.4 to 7.5 ± 0.4 pA; **Figure 6C, right panel**; t(13) = 4.03, p = 0.0014 by paired t-test, 1.16 ± 0.29 pA effect size with 95% confidence interval of -1.78 to -0.54). Together, these findings indicate that the δ subunit is expressed predominantly in CRF1- neurons whereas the α1 subunit is expressed predominantly in CRF1+ neurons, and that δ-containing $GABA_A$ receptors contribute to tonic conductance in CRF1- but not CRF1+ neurons.

Acute cellular ethanol exposure

$GABA_A$ receptors are sensitive to ethanol and tonic conductance has been shown to be selectively augmented by acute ethanol (Wallner et al., 2003; Wei et al., 2004; Herman et al., 2013). Focal application of ethanol (EtOH, 44 mM) did not significantly alter sIPSC inter-event interval or sIPSC frequency (107 ± 4.0 % of control; p = 0.1514 by one-sample t-test, n = 5 cells from 5 mice , **Figure 7A and 7C, top**) in CRF1+ neurons, but decreased inter-event interval and increased sIPSC frequency in CRF1- neurons [121.1 ± 1.3 % of control, n = 5 cells from 5 mice, **Figure 7B and 7C, top**; t(3) = 15.82, *p = 0.0005 by one-sample t-test; t(7) = 3.03, #p = 0.01915 by unpaired t-test; 14.08 ± 4.65 % control effect size with 95% confidence interval of -25.08 to -3.09]. Ethanol did not change sIPSC amplitude (97.76 ± 4.8 and 100.1 ± 4.3 % of

control, p = 0.7285 by unpaired t-test **Figure 7C, bottom**), rise (105.0 ± 5.8 and 105.6 ± 2.1 % of control, p = 0.9222 by unpaired t-test) or decay (104.5 ± 2.8 and 103.3 ± 2.2 % of control, p = 0.7395 by unpaired t-test) in CRF1+ or CRF1- neurons, respectively. Additionally, focal application of ethanol did not significantly change the holding current of CRF1+ neurons (1.2 ± 0.9 pA, n = 5 cells from 5 mice; **Figure 7D** and **Figure 7F**; p = 0.2304 by one-sample t-test), but did significantly increase holding current in CRF1- neurons (12.6 ± 0.9 pA, $t(4) = 14.11$, $^*p = 0.0001$ by one-sample t-test, n = 5 cells from 5 mice; $t(8) = 9.09$, $\#p = 0.0001$ by unpaired t-test, 11.37 ± 1.25 pA effect size with 95% confidence interval of -14.26 to -8.487; **Figure 7E** and **Figure 7F**). Acute ethanol did not significantly affect RMS noise in CRF1+ neurons (5.9 ± 0.2 pA at baseline to 6.1 ± 0.4 pA after EtOH, p = 0.3868) or CRF1- neurons (6.3 ± 0.5 pA at baseline to 6.2 ± 0.5 pA after EtOH, p = 0.6131).

Chronic Intermittent Ethanol Exposure

To examine the sensitivity of LA neurons to chronic ethanol exposure, we subjected CRF1:GFP mice to chronic intermittent ethanol (CIE) vapor exposure (4-5 weeks) and CIE followed by 3-7 days withdrawal (CIE-WD). There were no significant changes in membrane properties in CRF1+ neurons following ethanol vapor exposure or withdrawal (**Figure 8A**), and consistent with naïve neurons the majority of CRF1+ neurons from AIR, CIE, and CIE-WD mice exhibited spike accommodation (**Figure 8B**). Rheobase was reduced in CRF1+ neurons from CIE mice (74.74 ± 8.63 pA, n = 19 cells from 11 mice) as compared with neurons from AIR mice (46.15 ± 5.72 pA, n = 19 cells from 6 mice, $t(30) = 2.49$, p = 0.0187 by unpaired t-test, effect size -28.58 ± 11.49 pA with 95% confidence interval of -52.05 to -5.113; **Figure 8C, left**). Rheobase did not

462 significantly differ between CRF1+ neurons from CIE-WD mice (64 ± 11.85 pA, n = 10
463 cells from 3 mice) and neurons from AIR mice (p = 0.4708; **Figure 8C, left**). Threshold
464 to fire was also reduced in neurons from CIE mice (-58.58 ± 2.35 mV) versus neurons
465 from AIR mice (-49.71 ± 1.50 mV, $t(30) = 3.34$, p = 0.0022 via unpaired t-test, effect size
466 of 8.87 ± 2.65 mV with 95% confidence intervals of -14.29 to -3.46; **Figure 8C, right**)
467 but was not different in neurons from CIE-WD mice (-52.43 ± 2.55 mV) versus neurons
468 from AIR mice (p = 0.3353). In addition, we found no differences in action potentials
469 elicited by ascending current injection between the three exposure conditions (**Figure**
470 **8D**). Together, these findings indicate increases in excitability of LA CRF1+ neurons
471 following CIE exposure that are normalized under withdrawal conditions.

472 There were no significant changes in membrane properties in CRF1- neurons
473 following ethanol vapor exposure or withdrawal (**Figure 8E**), and consistent with
474 neurons from naïve mice approximately half of CRF1- neurons from AIR and CIE-WD
475 mice exhibited spike accommodation (**Figure 8F**). No changes in rheobase were
476 observed between CRF1- neurons from AIR mice (84.44 ± 12.37 pA, n = 9 cells from 4
477 mice), CIE mice (65.00 ± 7.32 pA, n = 8 cells from 3 mice) or CIE-WD mice (76.67 ±
478 26.03 pA, n = 6 cells from 3 mice; **Figure 8G, left**). Threshold to fire was also
479 comparable in CRF1- neurons from AIR mice (-50.18 ± 1.47 mV) versus neurons from
480 CIE mice (-48.00 ± 1.62 mV) and CIE-WD mice (-51.55 ± 1.76 mV; **Figure 8G, right**).
481 No significant differences in number of action potentials across current injection steps
482 emerged between CRF1- neurons from AIR, CIE or CIE-WD mice (**Figure 8H**). These
483 findings indicate no changes in excitability of CRF1- neurons following AIR, CIE or CIE-
484 WD exposure.

We next assessed phasic inhibitory transmission in CRF1+ and CRF1- LA neurons following vapor exposure. There were no significant changes in sIPSC frequency [5.4 ± 1.4 Hz, 7.1 ± 2.0 Hz, and 5.6 ± 1.2 Hz, p = 0.7112 by one-way ANOVA, n = 5-8 cells from 3-4 mice per group; **Figure 9A** and **9B, left panel**], sIPSC amplitude [67.0 ± 4.7 pA, 69.2 ± 3.4 pA, and 62.7 ± 5.5 pA, p = 0.6551 by one-way ANOVA, n = 5-8 cells from 3-4 mice per group; **Figure 9A** and **9B, center panel**], sIPSC rise [1.9 ± 1.1 ms, 1.8 ± 0.1 ms, and 1.9 ± 0.2 ms, p = 0.8369 by one-way ANOVA, n = 5-8 cells from 3-4 mice per group; **Figure 9A],** or sIPSC decay [1.9 ± 1.1 ms, 1.8 ± 0.1 ms, and 1.9 ± 0.2 ms, p = 0.9120 by one-way ANOVA, n = 5-8 cells from 3-4 mice per group; **Figure 9A** and **9B, right panel**] in CRF1+ neurons from AIR, CIE, and CIE-WD mice, respectively. CRF1- neurons from AIR, CIE, or CIE-WD mice were similarly unaffected. sIPSC frequency [5.4 ± 1.5 Hz, 5.7 ± 1.1 Hz, and 5.1 ± 1.9 Hz, p = 0.9761 by one-way ANOVA, n = 3-7 cells from 3 mice per group, **Figure 9C, left panel**], sIPSC amplitude [73.1 ± 5.0 pA, 72.2 ± 5.8 pA, and 65.6 ± 0.5 pA, p = 0.7758 by one-way ANOVA, n = 3-7 cells from 3 mice per group, **Figure 9C, center panel**], sIPSC rise [1.7 ± 0.7 ms, 1.1 ± 0.1 ms, and 1.0 ± 0.1 ms, p = 0.6595 by one-way ANOVA, n = 3-7 cells from 3 mice per group] and sIPSC decay [2.1 ± 0.1 ms, 1.8 ± 0.1 ms, and 2.4 ± 0.1 ms, p = 0.0902 by one-way ANOVA, n = 3-7 cells from 3 mice per group, **Figure 9C, right panel**] were all unchanged.

We also examined the tonic inhibitory conductance in CRF1+ and CRF1- neurons after CIE and CIE-WD. Focal application of gabazine (GBZ, 100 μM) produced a significant reduction in holding current that was not significantly different between CRF1+ neurons from AIR, CIE and CIE-WD mice [8.2 ± 1.4 pA, 11.1 ± 2.1 pA, and 8.7 ±

2.1 pA, p = 0.5122 by one-way ANOVA, n = 5-7 cells from 3-4 mice per group; **Figure 9D** and **9E**]. Gabazine (GBZ, 100 μM) also produced a reduction in the amplitude of the holding current or RMS noise that was not significantly different between CRF1+ neurons from AIR, CIE and CIE-WD mice [10.3 ± 0.5 to 8.8 ± 0.6 pA, 9.6 ± 0.7 to 8.3 ± 0.5 pA, and 9.3 ± 0.7 to 8.5 ± 0.9 pA; p = 0.4238 by one-way ANOVA, n = 5-7 cells from 3-4 mice per group]. Focal application of gabazine (GBZ, 100 μM) produced no reduction in holding current in CRF1- neurons from AIR, CIE or CIE-WD mice [0.7 ± 1.4 pA, 2.2 ± 1.4 pA, and 1.0 ± 3.6 pA, p = 0.7642 by one-way ANOVA, n = 3-7 cells from 3 mice per group; **Figure 9F**], no difference in the magnitude of reduction in the amplitude of the holding current or RMS noise [10.0 ± 0.7 to 9.1 ± 0.6 pA, 10.2 ± 0.9 to 8.8 ± 0.4 pA, and 7.8 ± 0.1 to 6.6 ± 0.4 pA, p = 0.6785 by one-way ANOVA, n = 3-7 cells from 3 mice per group] and no significant difference between the experimental groups. These data suggest tonic inhibitory signaling in the LA is insensitive to chronic ethanol exposure and chronic ethanol exposure followed by withdrawal.

In vivo microdialysis

To evaluate baseline transmitter levels following chronic ethanol exposure and withdrawal, we performed *in vivo* microdialysis in CRF1:GFP mice exposed to AIR (n = 4) or CIE-WD (n = 7). Mice were implanted with 0.5 mm microdialysis probes (**Figure 10A**) aimed at the LA. However, as some penetrance into BLA is possible, results are described as LA/BLA (**Figure 10B**). There were no significant differences detected between AIR and CIE-WD mice in basal GABA levels (9.2 ± 2.1 nM and 11.9 ± 1.3 nM, p = 0.28 by unpaired t-test n = 4-7; **Figure 10C**). Acute administration of ethanol (1 M) in the perfusate solution produced significant increases in LA/BLA GABA levels in both

AIR and CIE-WD mice as assessed by two-way ANOVA of pre and post-ethanol reverse dialysis (exposure condition X time) with a significant main effect of time, $F(11, 99) = 5.585$, $p = 0.0001$, but no significant effect of exposure condition or interaction of time and exposure condition (**Figure 10D**). There were also no significant differences detected between AIR and CIE-WD mice in basal glutamate levels (1264 ± 310.5 nM and 1061 ± 295.8 nM, $p = 0.67$, n = 4- 7; **Figure 10E**). Acute administration of ethanol (1 M in the perfusate solution) produced significant increases in LA/BLA glutamate levels in both AIR and CIE-WD mice as assessed by two-way ANOVA of pre and post-ethanol reverse dialysis (exposure condition X time) with a significant main effect of time, $F(11, 99) = 4.747$, $p = 0.0001$, but no significant effect of exposure condition or interaction of time and exposure condition (**Figure 10F**). These data suggest that baseline excitatory and inhibitory transmitter levels in the LA/BLA are not significantly altered by chronic ethanol exposure and withdrawal, and that the responsivity of these transmitter systems to ethanol also remains intact following chronic ethanol exposure and withdrawal.

DISCUSSION

The CRF1 system in the amygdala has been shown to play an important role in the development of ethanol dependence, but the CRF1-containing neuronal population specifically within the LA has not been fully characterized. Here, we report that CRF1+ neurons in the LA are composed of multiple subgroups, including a small percentage of neurons expressing calcium binding proteins and a larger percentage of glutamatergic neurons. CRF1+ neurons exhibit distinct membrane properties, minor differences in baseline excitability and possess an ongoing tonic $GABA_A$ receptor conductance that

554 CRF1- neurons lack. Acute ethanol exposure increases inhibition of CRF1- neurons but
555 the inhibitory control of CRF1+ neurons is insensitive to acute ethanol. CRF1+ neurons
556 displayed increased excitability following chronic ethanol, however neither CRF1+ nor
557 CRF1- LA cells displayed alterations in phasic or tonic GABAergic synaptic transmission
558 following chronic ethanol exposure or withdrawal, nor were basal changes in
559 extracellular GABA or glutamate levels observed between exposure groups.
560 Collectively, these results suggest that CRF1- LA neurons are sensitive to acute ethanol
561 but that changes in CRF1+ neuronal excitability following chronic ethanol are not due to
562 neuroplastic changes in inhibitory control.

563 Both phasic and tonic GABAergic signaling regulate the activity and output of
564 amygdala neurons. CRF1+ LA cells exhibit heightened basal phasic GABAergic
565 signaling as compared with CRF1- cells and an ongoing tonic conductance that CRF1-
566 cells lack. Subunit stoichiometry regulates the ability of $GABA_A$ receptors to mediate
567 tonic inhibition, with the δ, α5 and ε subunits imparting sensitivity of $GABA_A$ receptors to
568 low levels of GABA that are thought to underlie tonic conductance (Stell and Mody,
569 2002; Stell et al., 2003; Glykys and Mody, 2007).The results of the
570 immunohistochemical studies indicate that CRF1+ cells predominantly express the α1
571 subunit and exhibit little colocalization with the δ subunit, consistent with previous
572 reports (Wiltgen et al., 2009). Consistent with this observation, the tonic conductance
573 seen in this population was insensitive to application of the δ-preferring $GABA_A$ receptor
574 agonist THIP. The tonic $GABA_A$ receptors in CRF1+ cells of the LA therefore do not
575 contain δ subunits but may contain alternative subunit stoichiometry, such as α1β2γ2 or
576 α5βγ2. In the CeA, the tonic conductance exhibited by CRF1+ neurons was enhanced

by the application of the preferential α1 $GABA_A$ agonist zolpidem, suggesting a role for α1-containing $GABA_A$ receptors in tonic inhibition in that population. A similar mechanism may regulate tonic conductance in LA CRF1+ neurons. The δ subunit was sparsely expressed in unlabeled LA cells, as seen previously (Pirker et al., 2000), and a tonic conductance in CRF1- neurons was stimulated by acute application of THIP. These findings suggest that CRF1- cells express δ subunit-containing $GABA_A$ receptors that are not active under basal conditions but may be stimulated by agonist activity or heightened concentrations of extracellular GABA.

Previous research has assessed the effects of ethanol on inhibitory signaling within the LA/BLA broadly, but the effects of ethanol on GABAergic signaling and within specific CRF1+ and CRF1- populations have not been previously assessed. We observed that CRF1+ cells are relatively insensitive to changes in inhibitory control induced by acute ethanol; focal application failed to elicit a change in either phasic or tonic inhibitory signaling in this population. As CRF1+ neurons exhibited heightened phasic and tonic $GABA_A$ signaling, these results may suggest a ceiling effect that precludes the possibility of GABA-mimetics such as ethanol from further increasing sIPSC frequency or reducing holding current. In contrast, CRF1- cells demonstrated an increased tonic conductance in the presence of ethanol coupled with a significant increase in GABA release onto these cells. These differences in sensitivity to acute ethanol may be related to $GABA_A$ subunit expression differences between the two populations. δ-containing $GABA_A$ receptors have heightened sensitivity to ethanol (Wallner et al., 2003; Wei et al., 2004), and the δ-expressing CRF1- neurons exhibited increases in tonic inhibitory control in response to ethanol that the δ-lacking CRF1+

cells failed to demonstrate. The insensitivity of CRF1+ cells to acute ethanol was also observed in the CeA (Herman et al., 2013), suggesting that this population may have similar $GABA_A$ receptor compositions in multiple amygdala nuclei.

In contrast to the selective effects of acute ethanol, both phasic and tonic $GABA_A$ signaling in LA CRF1+ and CRF1- cells were not affected by chronic ethanol exposure or ethanol exposure and withdrawal. The microdialysis experiments showed that chronic ethanol and withdrawal did not produce adaptations in extracellular GABA or glutamate levels, which may explain the insensitivity of tonic conductance in CRF1- neurons to ethanol-induced adaptations. Chronic ethanol exposure has been shown to increase basal GABA concentration in the CeA (Roberto et al., 2004a), elevating ambient GABA that is thought to drive cell type-specific changes in inhibitory control (Herman et al., 2016). Although the $GABA_A$ receptor subunits associated with CRF1+ and CRF1- neurons in the CeA and LA are similar, the lack of elevated ambient GABA in the LA likely precludes any chronic ethanol-induced plasticity in inhibitory signaling in either CRF1+ or CRF1- LA neurons. Together, these findings may suggest that unlike the CeA, inhibitory control of CRF1+ neurons in the LA is relatively preserved following chronic ethanol exposure.

Importantly, following chronic ethanol exposure CRF1+ neurons displayed reductions in the rheobase and threshold to fire, indicating increased excitability of CRF1+ neurons but not CRF1- neurons. Thus, although inhibitory signaling in CRF1+ population is relatively insensitive to the effects of acute ethanol, it is sensitive to chronic ethanol in multiple amygdala nuclei (the CeA and LA), making the CRF1+ population an important target for the actions of ethanol broadly within the amygdala.

623 The results of the voltage clamp experiments suggest that this enhanced excitability in
624 the CRF1+ population is not driven by alterations in GABAergic signaling, which may
625 indicate that these changes are instead regulated by ethanol-induced alterations in
626 intrinsic excitability within the LA. Plasticity in glutamatergic signaling within the LA/BLA
627 has been reported following chronic ethanol exposure (McCool et al., 2010), and the LA
628 specifically exhibits alterations in molecular markers of glutamate signaling following
629 chronic ethanol exposure in nonhuman primates (Alexander et al., 2018) and
630 reinstatement of alcohol seeking in mice (Salling et al., 2017). Future work to
631 characterize glutamatergic signaling in the CRF1+ and CRF1- populations of the LA
632 both under basal conditions and following chronic ethanol exposure would help to clarify
633 the mechanisms underlying these ethanol-induced changes in excitability.

634 In the chronic vapor exposure experiments, we did not find evidence for
635 increased baseline phasic GABAergic signaling in CRF1+ versus CRF1- cells that was
636 observed in our experiments with naïve mice. The baseline sIPSC frequency in CRF1+
637 neurons from AIR, CIE, and CIE-WD mice was lower than what was observed in CRF1+
638 neurons from naïve mice and higher in CRF1- neurons from AIR, CIE, and CIE-WD
639 mice (see **Figure 4A and B** and **Figure 9B and C**), collectively leading to a loss of
640 significant differences between the two cell populations in the chronic ethanol exposure
641 experiments. As our data indicate that the CRF1+ cell population is comprised of a
642 majority of glutamatergic principal neurons and a smaller subpopulation of interneurons,
643 it is possible that differences in cell subpopulations sampled between the two
644 experiments could account for these different baseline characteristics. However, we did
645 observe tonic inhibition in the CRF1+ population and not the CRF1- population in slices

from both naïve and vapor-exposed mice, which suggests that a similar population of cells was sampled in both sets of experiments. The loss of population differences in phasic but not tonic inhibition may be attributable to the stress of repeated injection, as the air-exposed mice were given daily pyrazole injections as a control for the treatment given to the CIE and CIE-WD groups. It is also possible that exposure to the air chamber, which as a novel environment may be a mild stressor, contributed to the differences between naïve and AIR mice in these experiments. The relative sensitivity of phasic and tonic inhibitory control in CRF1+ cells to repeated mild stress is an interesting avenue for future studies to explore.

Together, these findings suggest that unlike adaptations in inhibitory control exhibited by other amygdala nuclei (notably the CeA), GABAergic signaling within the LA is intact despite chronic ethanol exposure and/or withdrawal. This resistance to ethanol-induced plasticity in inhibitory control within the LA may play a significant role in the development of alcohol dependence and alcohol use disorders. Sensory information, including external drug cues and internal states such as craving and withdrawal, is relayed first to the LA from the cortex and thalamus; glutamatergic projections from the LA then synapse with cells in the CeA, BLA and Ipc (Sah et al., 2003). Our findings suggest that despite chronic ethanol exposure, inhibitory control of LA CRF1+ neurons (many of which are projection neurons) remains unchanged, allowing these cells to communicate with downstream amygdalar regions unimpeded. This suggests that neuroadaptations developing in the CeA (Herman et al., 2016) and BLA (Lack et al., 2007; Diaz et al., 2011) upon chronic ethanol exposure result from local, intrinsic changes rather than from changes in extrinsic inputs from the LA. These

findings may have relevance to amygdala circuitry in other contexts, such as fear learning, and may provide insights into other diseases involving amygdala dysfunction, including anxiety and depression. These findings also highlight the heterogeneous cell types within the LA and underscore the need for further cell type-specific characterization of amygdala physiology and pathology.

675 **REFERENCES**

676 Agoglia AE, Herman MA (2018) The center of the emotional universe: Alcohol, stress,
677 and CRF1 amygdala circuitry. Alcohol 72:61-73.
678 Alexander NJ, Rau AR, Jimenez VA, Daunais JB, Grant KA, McCool BA (2018) SNARE
679 Complex-Associated Proteins in the Lateral Amygdala of Macaca mulatta
680 Following Long-Term Ethanol Drinking. Alcohol Clin Exp Res 42:1661-1673.
681 Baur R, Kaur KH, Sigel E (2009) Structure of alpha6 beta3 delta GABA(A) receptors
682 and their lack of ethanol sensitivity. J Neurochem 111:1172-1181.
683 Belelli D, Harrison NL, Maguire J, Macdonald RL, Walker MC, Cope DW (2009)
684 Extrasynaptic GABAA receptors: form, pharmacology, and function. J Neurosci
685 29:12757-12763.
686 Borghese CM, Harris RA (2007) Studies of ethanol actions on recombinant delta-
687 containing gamma-aminobutyric acid type A receptors yield contradictory results.
688 Alcohol 41:155-162.
689 Buczynski MW, Herman MA, Hsu KL, Natividad LA, Irimia C, Polis IY, Pugh H, Chang
690 JW, Niphakis MJ, Cravatt BF, Roberto M, Parsons LH (2016) Diacylglycerol
691 lipase disinhibits VTA dopamine neurons during chronic nicotine exposure. Proc
692 Natl Acad Sci U S A 113:1086-1091.
693 Calakos KC, Blackman D, Schulz AM, Bauer EP (2017) Distribution of type I
694 corticotropin-releasing factor (CRF1) receptors on GABAergic neurons within the
695 basolateral amygdala. Synapse 71.

696 Diaz MR, Christian DT, Anderson NJ, McCool BA (2011) Chronic ethanol and
697 withdrawal differentially modulate lateral/basolateral amygdala paracapsular and
698 local GABAergic synapses. J Pharmacol Exp Ther 337:162-170.
699 Eckardt MJ, File SE, Gessa GL, Grant KA, Guerri C, Hoffman PL, Kalant H, Koob GF, Li
700 TK, Tabakoff B (1998) Effects of moderate alcohol consumption on the central
701 nervous system. Alcohol Clin Exp Res 22:998-1040.
702 Glykys J, Mody I (2007) Activation of GABAA receptors: views from outside the synaptic
703 cleft. Neuron 56:763-770.
704 Grobin AC, Matthews DB, Devaud LL, Morrow AL (1998) The role of GABA(A)
705 receptors in the acute and chronic effects of ethanol. Psychopharmacology (Berl)
706 139:2-19.
707 Herman MA, Contet C, Roberto M (2016) A Functional Switch in Tonic GABA Currents
708 Alters the Output of Central Amygdala Corticotropin Releasing Factor Receptor-1
709 Neurons Following Chronic Ethanol Exposure. J Neurosci 36:10729-10741.
710 Herman MA, Contet C, Justice NJ, Vale W, Roberto M (2013) Novel subunit-specific
711 tonic GABA currents and differential effects of ethanol in the central amygdala of
712 CRF receptor-1 reporter mice. J Neurosci 33:3284-3298.
713 Hubbard DT, Nakashima BR, Lee I, Takahashi LK (2007) Activation of basolateral
714 amygdala corticotropin-releasing factor 1 receptors modulates the consolidation
715 of contextual fear. Neuroscience 150:818-828.
716 Justice NJ, Yuan ZF, Sawchenko PE, Vale W (2008) Type 1 corticotropin-releasing
717 factor receptor expression reported in BAC transgenic mice: implications for

718 reconciling ligand-receptor mismatch in the central corticotropin-releasing factor
719 system. J Comp Neurol 511:479-496.
720 Koob GF, Roberts AJ, Schulteis G, Parsons LH, Heyser CJ, Hyytia P, Merlo-Pich E,
721 Weiss F (1998) Neurocircuitry targets in ethanol reward and dependence.
722 Alcohol Clin Exp Res 22:3-9.
723 Krook-Magnuson EI, Huntsman MM (2005) Excitability of cortical neurons depends
724 upon a powerful tonic conductance in inhibitory networks. Thalamus Relat Syst
725 3:115-120.
726 Lack AK, Diaz MR, Chappell A, DuBois DW, McCool BA (2007) Chronic ethanol and
727 withdrawal differentially modulate pre- and postsynaptic function at glutamatergic
728 synapses in rat basolateral amygdala. J Neurophysiol 98:3185-3196.
729 Lovinger DM, Roberto M (2013) Synaptic effects induced by alcohol. Curr Top Behav
730 Neurosci 13:31-86.
731 Marowsky A, Rudolph U, Fritschy JM, Arand M (2012) Tonic inhibition in principal cells
732 of the amygdala: a central role for alpha3 subunit-containing GABAA receptors. J
733 Neurosci 32:8611-8619.
734 McCool BA, Christian DT, Diaz MR, Lack AK (2010) Glutamate plasticity in the drunken
735 amygdala: the making of an anxious synapse. Int Rev Neurobiol 91:205-233.
736 Mody I, Glykys J, Wei W (2007) A new meaning for "Gin & Tonic": tonic inhibition as the
737 target for ethanol action in the brain. Alcohol 41:145-153.
738 Nie Z, Schweitzer P, Roberts AJ, Madamba SG, Moore SD, Siggins GR (2004) Ethanol
739 augments GABAergic transmission in the central amygdala via CRF1 receptors.
740 Science 303:1512-1514.

741 Overstreet DH, Knapp DJ, Breese GR (2004) Modulation of multiple ethanol withdrawal-
742 induced anxiety-like behavior by CRF and CRF1 receptors. Pharmacol Biochem
743 Behav 77:405-413.
744 Pavon FJ, Serrano A, Sidhpura N, Polis I, Stouffer D, de Fonseca FR, Cravatt BF,
745 Martin-Fardon R, Parsons LH (2018a) Fatty acid amide hydrolase (FAAH)
746 inactivation confers enhanced sensitivity to nicotine-induced dopamine release in
747 the mouse nucleus accumbens. Addict Biol 23:723-734.
748 Pavon FJ, Serrano A, Stouffer DG, Polis I, Roberto M, Cravatt BF, Martin-Fardon R,
749 Rodriguez de Fonseca F, Parsons LH (2018b) Ethanol-induced alterations in
750 endocannabinoids and relevant neurotransmitters in the nucleus accumbens of
751 fatty acid amide hydrolase knockout mice. Addict Biol.
752 Pirker S, Schwarzer C, Wieselthaler A, Sieghart W, Sperk G (2000) GABA(A) receptors:
753 immunocytochemical distribution of 13 subunits in the adult rat brain.
754 Neuroscience 101:815-850.
755 Pitkanen A, Savander V, LeDoux JE (1997) Organization of intra-amygdaloid circuitries
756 in the rat: an emerging framework for understanding functions of the amygdala.
757 Trends Neurosci 20:517-523.
758 Rainnie DG, Bergeron R, Sajdyk TJ, Patil M, Gehlert DR, Shekhar A (2004)
759 Corticotrophin releasing factor-induced synaptic plasticity in the amygdala
760 translates stress into emotional disorders. J Neurosci 24:3471-3479.
761 Roberto M, Madamba SG, Stouffer DG, Parsons LH, Siggins GR (2004a) Increased
762 GABA release in the central amygdala of ethanol-dependent rats. J Neurosci
763 24:10159-10166.

764 Roberto M, Schweitzer P, Madamba SG, Stouffer DG, Parsons LH, Siggins GR (2004b)
765 Acute and chronic ethanol alter glutamatergic transmission in rat central
766 amygdala: an in vitro and in vivo analysis. J Neurosci 24:1594-1603.
767 Roberto M, Cruz MT, Gilpin NW, Sabino V, Schweitzer P, Bajo M, Cottone P, Madamba
768 SG, Stouffer DG, Zorrilla EP, Koob GF, Siggins GR, Parsons LH (2010)
769 Corticotropin releasing factor-induced amygdala gamma-aminobutyric Acid
770 release plays a key role in alcohol dependence. Biol Psychiatry 67:831-839.
771 Rodrigues SM, Schafe GE, LeDoux JE (2004) Molecular mechanisms underlying
772 emotional learning and memory in the lateral amygdala. Neuron 44:75-91.
773 Rostkowski AB, Leitermann RJ, Urban JH (2013) Differential activation of neuronal cell
774 types in the basolateral amygdala by corticotropin releasing factor.
775 Neuropeptides 47:273-280.
776 Sah P, Faber ES, Lopez De Armentia M, Power J (2003) The amygdaloid complex:
777 anatomy and physiology. Physiol Rev 83:803-834.
778 Salling MC, Hodge CJ, Psilos KE, Eastman VR, Faccidomo SP, Hodge CW (2017) Cue-
779 induced reinstatement of alcohol-seeking behavior is associated with increased
780 CaMKII T286 phosphorylation in the reward pathway of mice. Pharmacol
781 Biochem Behav 163:20-29.
782 Saxena NC, Macdonald RL (1996) Properties of putative cerebellar gamma-
783 aminobutyric acid A receptor isoforms. Mol Pharmacol 49:567-579.
784 Sears RM, Schiff HC, LeDoux JE (2014) Molecular mechanisms of threat learning in the
785 lateral nucleus of the amygdala. Prog Mol Biol Transl Sci 122:263-304.

786 Semyanov A, Walker MC, Kullmann DM, Silver RA (2004) Tonically active GABA A
787 receptors: modulating gain and maintaining the tone. Trends Neurosci 27:262-
788 269.
789 Song P, Mabrouk OS, Hershey ND, Kennedy RT (2012) In vivo neurochemical
790 monitoring using benzoyl chloride derivatization and liquid chromatography-mass
791 spectrometry. Anal Chem 84:412-419.
792 Sosulina L, Meis S, Seifert G, Steinhauser C, Pape HC (2006) Classification of
793 projection neurons and interneurons in the rat lateral amygdala based upon
794 cluster analysis. Mol Cell Neurosci 33:57-67.
795 Stell BM, Mody I (2002) Receptors with different affinities mediate phasic and tonic
796 GABA(A) conductances in hippocampal neurons. J Neurosci 22:RC223.
797 Stell BM, Brickley SG, Tang CY, Farrant M, Mody I (2003) Neuroactive steroids reduce
798 neuronal excitability by selectively enhancing tonic inhibition mediated by delta
799 subunit-containing GABAA receptors. Proc Natl Acad Sci U S A 100:14439-
800 14444.
801 Tye KM, Prakash R, Kim SY, Fenno LE, Grosenick L, Zarabi H, Thompson KR,
802 Gradinaru V, Ramakrishnan C, Deisseroth K (2011) Amygdala circuitry mediating
803 reversible and bidirectional control of anxiety. Nature 471:358-362.
804 Ugolini A, Sokal DM, Arban R, Large CH (2008) CRF1 receptor activation increases the
805 response of neurons in the basolateral nucleus of the amygdala to afferent
806 stimulation. Front Behav Neurosci 2:2.

807 Van Pett K, Viau V, Bittencourt JC, Chan RK, Li HY, Arias C, Prins GS, Perrin M, Vale
808 W, Sawchenko PE (2000) Distribution of mRNAs encoding CRF receptors in
809 brain and pituitary of rat and mouse. J Comp Neurol 428:191-212.
810 Wallner M, Hanchar HJ, Olsen RW (2003) Ethanol enhances alpha 4 beta 3 delta and
811 alpha 6 beta 3 delta gamma-aminobutyric acid type A receptors at low
812 concentrations known to affect humans. Proc Natl Acad Sci U S A 100:15218-
813 15223.
814 Wei W, Faria LC, Mody I (2004) Low ethanol concentrations selectively augment the
815 tonic inhibition mediated by delta subunit-containing GABAA receptors in
816 hippocampal neurons. J Neurosci 24:8379-8382.
817 Weiner JL, Valenzuela CF (2006) Ethanol modulation of GABAergic transmission: the
818 view from the slice. Pharmacol Ther 111:533-554.
819 Wiltgen BJ, Godsil BP, Peng Z, Saab F, June HL, Linn ML, Cook JM, Houser CR, O'Dell
820 TJ, Homanics GE, Fanselow MS (2009) The alpha1 subunit of the GABA(A)
821 receptor modulates fear learning and plasticity in the lateral amygdala. Front
822 Behav Neurosci 3:37.

823

FIGURE LEGENDS

Figure 1. Glutamate transporter expression in CRF1 lateral amygdala neurons. (**A**) Representative merged image showing *Crhr1, Gfp* and DAPI in the LA. Scale bar = 10 µm. (**B**) Summary of the total number of *Gfp*+ and *Crhr1*+ nuclei in the ROI (1024X1024, 40X) in the LA of 11 images from 3 mice. (**C**) Graph of the percent of nuclei co-expressing *Crhr1* in *Gfp*+ nuclei (black bar) and percent of nuclei co-expressing *Gfp* in *Crhr1*+ nuclei (white bar). Representative images in the LA are shown for (**D**) *Crhr1* and DAPI, (**E**) *Slc17a7* and DAPI, and (**F**) the merged imaged of *Crhr1*, *Slc17a7*, and DAPI (*Crhr1* = red fluorescence, *Slc17a7* = green fluorescence, and DAPI = blue fluorescence). Scale bar = 10 µm. (**G**) Summary of the total number of *Crhr1*+ and *Slc17a7*+ nuclei in the ROI (1024X1024, 40X) in the LA of 10 images from 3 CRF1:GFP mice. (**H**) Graph of the percent of nuclei co-expressing *Crhr1* in *Slc17a7*+ nuclei (black bar) and nuclei co-expressing *Slc17a7* in *Crhr1*+ (white bar).

Figure 2. Calcium binding protein expression in CRF1+ and CRF1- lateral amygdala neurons. (**A**) Photomicrograph (10x) of GFP expression (green fluorescence, left), calbindin expression (red fluorescence, center) and merge (right). Scale bar = 100 µm. (**B**) Photomicrograph (10x) of GFP expression (green fluorescence, left), calretinin expression (red fluorescence, center) and merge (right). Scale bar = 100 µm. (**C**) Photomicrograph (10x) of GFP expression (green fluorescence, left), parvalbumin expression (red fluorescence, center) and merge (right). Scale bar = 100 µm. (**D**) Summary of total cells expressing CRF1 (GFP) and calcium binding proteins (CBPs), n = 16 sections from 4 mice. (**E**) Percent of CBP+ cells that co-express CRF1. (**F**) Percent of CRF1+ cells that co-express CBPs.

847 **Figure 3. Membrane characteristics and excitability of CRF1+ and CRF1- lateral**
848 **amygdala neurons.** (**A**) Summary of membrane characteristics of CRF1+ (n = 28) and
849 CRF1- (n = 28) LA cells. (**B**) Representative current-clamp recording of LA CRF1+
850 neuron action potentials elicited by 100 pA current injection (**top**) and the relative
851 proportion of CRF1+ LA neurons displaying spike accommodation with current injection
852 (**bottom**). (**C**) Representative current-clamp recording of LA CRF1- neuron action
853 potentials elicited by 100 pA current injection (**top**) and the relative proportion of CRF1-
854 LA neurons displaying spike accommodation with current injection (**bottom**). (**D**)
855 Summary of rheobase at -70 mV (**left**) and threshold to fire (**right**) of CRF1+ and CRF1-
856 LA neurons. *$p < 0.05$ by unpaired t test comparing CRF1+ to CRF1− cells. (**E)**
857 Summary of action potentials by current injection in CRF1+ and CRF1- LA neurons.

858 **Figure 4. Phasic and tonic inhibitory transmission in CRF1 lateral amygdala**
859 **neurons.** (**A**) Representative voltage-clamp recording of a CRF1+ cell (**left**) and a
860 CRF1- cell (**right**). (**B**) Summary of sIPSC frequency (**left**), amplitude (**center**) and
861 decay (**right**) of CRF1+ and CRF1- cells. *$p < 0.05$ by unpaired t test comparing
862 CRF1+ to CRF1− cells. (**C**) Representative voltage-clamp recording of a CRF1+ cell
863 (**left**) and a CRF1- cell (**right**) during gabazine superfusion (GBZ, 100μM). White
864 dashed line indicates level of holding current before and after GBZ superfusion. (**D**)
865 Summary of the tonic current revealed by gabazine. *$p < 0.05$ by unpaired t test
866 comparing CRF1+ to CRF1− cells. (**E**) Summary of the change in RMS noise induced
867 by gabazine superfusion in CRF1+ (**left**) and CRF1- (**right**) cells.

868 **Figure 5. $GABA_A$ subunit expression in CRF1+ and CRF1- lateral amygdala**
869 **neurons.** (**A**) Photomicrograph (10x) of GFP expression (green fluorescence) in LA. (**B**)

Photomicrograph (10x) of α1 $GABA_A$ receptor subunit expression (red fluorescence) in LA. Scale bar = 100 μm. (**C**) Photomicrograph (60x) of GFP expression (**top**), α1 expression (**center**) and merge (bottom) in LA highlighting a single cell exhibiting coexpression of GFP and α1. Scale bar = 10 μm. (**D**) Photomicrograph (10x) of GFP expression (green fluorescence) in LA. (**E**) Photomicrograph (10x) of δ $GABA_A$ receptor subunit expression (red fluorescence) in LA. Scale bar = 100 μm. (**F**) Photomicrograph (60x) of GFP expression (**top**), δ expression (**center**) and merge (**bottom**) in LA. Scale bar = 10 μm.

Figure 6. Contribution of δ subunit-containing $GABA_A$ receptors to tonic conductance in CRF1+ and CRF1- lateral amygdala neurons.(**A**) Representative voltage-clamp recording of a CRF1+ (**left**) and CRF1- (**right**) cell during superfusion of the δ subunit-preferring $GABA_A$ agonist gaboxadol (THIP, 5 μM). White dashed line indicates level of holding current before and after THIP superfusion. (**B**) Summary of the tonic current induced by THIP in CRF1+ and CRF1- cells, $*p < 0.05$ by unpaired t test comparing CRF1+ to CRF1− cells. (**C**) Summary of the change in RMS noise induced by THIP superfusion in CRF1+ (**left**) and CRF1- (**right**) cells.

Figure 7. Effects of acute ethanol on phasic and tonic inhibitory transmission in CRF1+ and CRF1- lateral amygdala neurons. (**A**) Representative voltage-clamp recording (**top**) and cumulative probability histogram of inter-event interval (**bottom**) of a CRF1+ cell during superfusion of ethanol (EtOH, 44mM). (**B**) Representative voltage-clamp recording (**top**) and cumulative probability histogram of inter-event interval (**bottom**) of a CRF1- cell during superfusion of ethanol (EtOH, 44mM). (**C**) Summary of the change in sIPSC frequency (**top**) and amplitude (**bottom**) following ethanol

superfusion as compared with baseline in CRF1+ and CRF1- cells. *$p < 0.05$ by one sample t test comparing differences from baseline within cell type, # $p < 0.05$ by unpaired t test comparing CRF1+ to CRF1- cells. (**D**) Representative voltage-clamp recording of a CRF1+ cell during superfusion of ethanol (EtOH, 44mM). White dashed line indicates level of holding current before and after EtOH superfusion. (**E**) Representative voltage-clamp recording of a CRF1- cell during superfusion of ethanol (EtOH, 44mM). White dashed line indicates level of holding current before and after EtOH superfusion. (**F**) Summary of the tonic current induced by ethanol in CRF1+ and CRF1- cells. *$p < 0.05$ by one sample t test comparing differences from baseline within cell type, # $p < 0.05$ by unpaired t test comparing CRF1+ to CRF1- cells.

Figure 8. Effects of chronic ethanol vapor on membrane characteristics and excitability in CRF1+ and CRF1- lateral amygdala neurons. (**A**) Summary of membrane characteristics of CRF1+ LA neurons from AIR, CIE, and CIE-WD mice. (**B**) Relative proportion of CRF1+ neurons exhibiting spike accommodation from control (AIR, **left**), chronic ethanol exposure (CIE, **center**) and chronic ethanol exposure and withdrawal (CIE-WD, **right**) mice. (**C**) Summary of rheobase at -70 mV (left) and threshold to fire (**right**) of CRF1+ neurons from AIR, CIE and CIE-WD mice. *$p < 0.05$ by unpaired t test comparing CRF1+ neurons from AIR mice to CRF1+ neurons from CIE mice. (**D)** Summary of action potentials by current injection in CRF1+ neurons from AIR, CIE and CIE-WD mice. (**E**) Summary of membrane characteristics of CRF1- LA neurons from AIR, CIE, and CIE-WD mice. (**F**) Relative proportion of CRF1- neurons exhibiting spike accommodation from AIR (**left**), CIE (**center**) and CIE-WD (**right**) mice. (**G**) Summary of rheobase at -70 mV (**left**) and threshold to fire (**right**) of CRF1-

neurons from AIR, CIE and CIE-WD mice. (**H)** Summary of action potentials by current injection in CRF1- neurons from AIR, CIE and CIE-WD mice.

Figure 9. Effects of chronic ethanol vapor on phasic and tonic inhibitory transmission in CRF1+ and CRF1- lateral amygdala neurons. (**A**) Representative voltage-clamp recordings of CRF1+ neurons from control (AIR, **left**), chronic ethanol exposure (CIE, **center**) and chronic ethanol exposure and withdrawal (CIE-WD, **right**) mice. (**B**) Summary of sIPSC frequency (**left**), amplitude (**center**) and decay (**right**) in CRF1+ neurons from AIR, CIE and CIE-WD mice. (**C**) Summary of sIPSC frequency (**left**), amplitude (**center**) and decay (**right**) in CRF1- neurons from AIR, CIE and CIE-WD mice. (**D**) Representative voltage-clamp recording of CRF1+ cells from AIR (**left**) and CIE-WD (**right**) mice during gabazine superfusion (GBZ, 100μM). White dashed line indicates level of holding current before and after GBZ superfusion. (**E**) Summary of tonic current revealed by gabazine superfusion in CRF1+ cells. (**F**) Summary of tonic current revealed by gabazine superfusion in CRF1- cells.

Figure 10. Effects of chronic ethanol vapor and withdrawal on exogenous GABA and glutamate concentration and sensitivity to acute ethanol in lateral amygdala/basolateral amygdala. (**A**) Representative microdialysis probe (0.5 mm). Scale bar = 1mm. (**B**) Histological verification of probe site. Dashed lines indicate LA/BLA. Scale bar = 1 mm. (**C**) Baseline dialysate concentrations of GABA (nM) in the LA/BLA of control (AIR) and chronic ethanol withdrawal (CIE-WD) mice (n=4-7). (**D**) Percentage change in GABAergic transmission in the LA/BLA of AIR over time and following reverse dialysis of ethanol (1 M, shaded area) in AIR and CIE-WD mice (n=4-7). (**E**) Baseline dialysate levels of glutamate (nM) in the LA/BLA of control (AIR) and

939 chronic ethanol and withdrawal (CIE-WD) mice (n=4-7). (**F**) Percentage change in
940 glutamatergic transmission in the LA/BLA over time and following reverse dialysis of
941 ethanol (1 M, shaded area) in AIR and CIE-WD mice (n = 4-7).

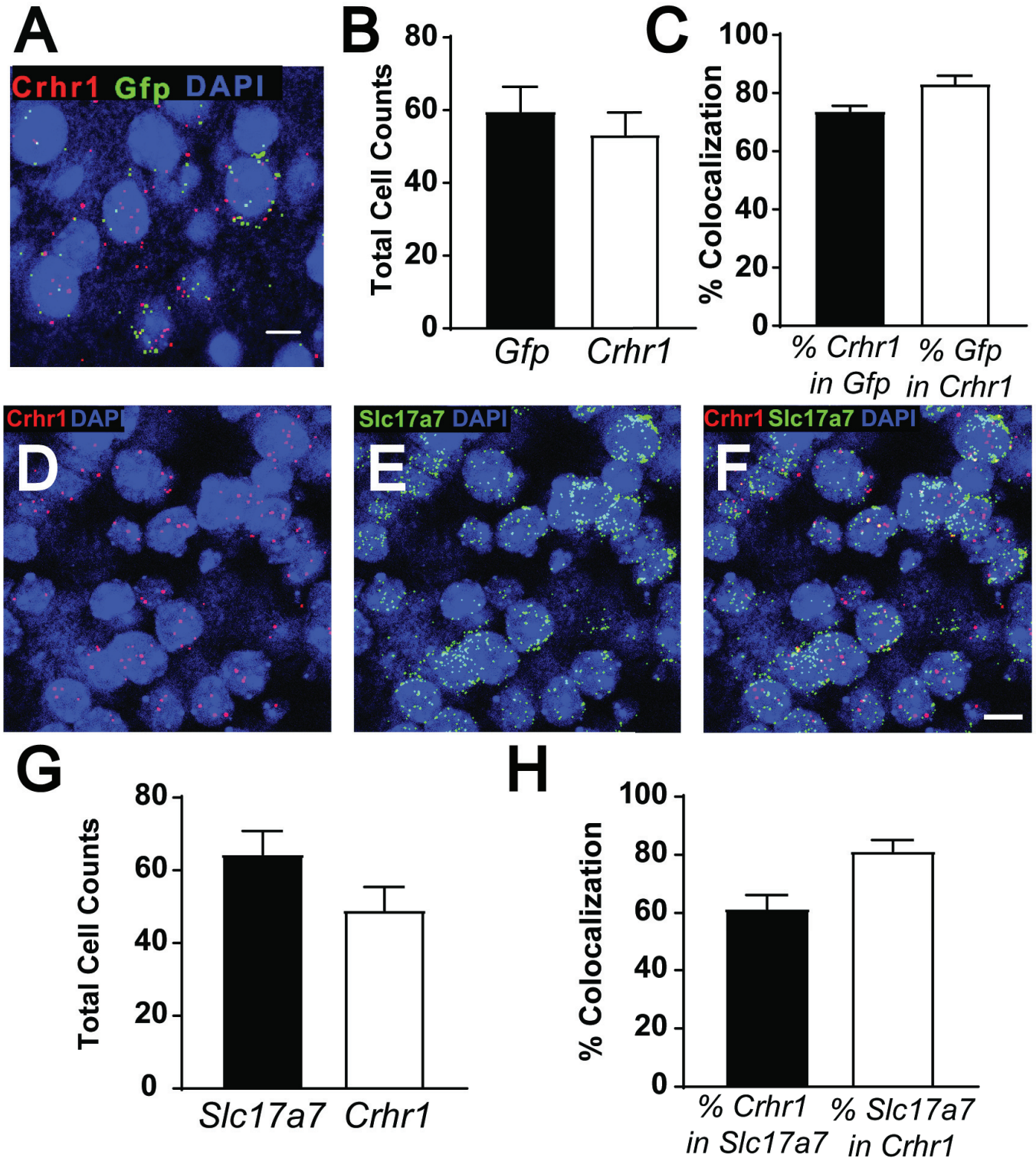

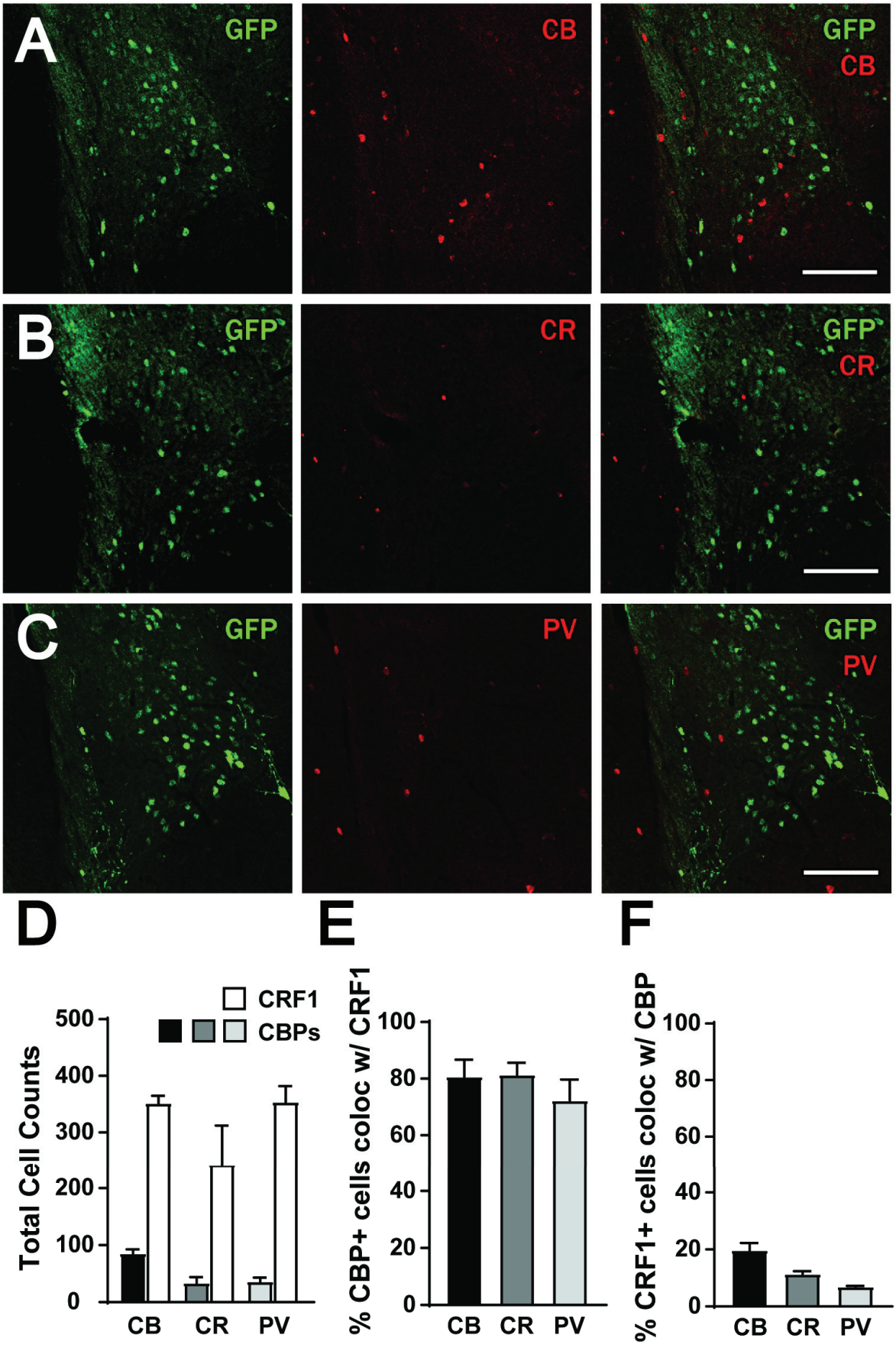

A	Membrane Capacitance Cm (pF)	Membrane Resistance Rm (MΩ)	Time Constant Tau (ms)	Membrane Potential Vm (mV)
CRF1+	52.0 ± 3.4*	172.2 ± 25.1*	375.5 ± 37.9*	-58.9 ± 1.8*
CRF1-	73.9 ± 6.6	122.7 ± 15.1	601.7 ± 63.1	-68.0 ± 1.4

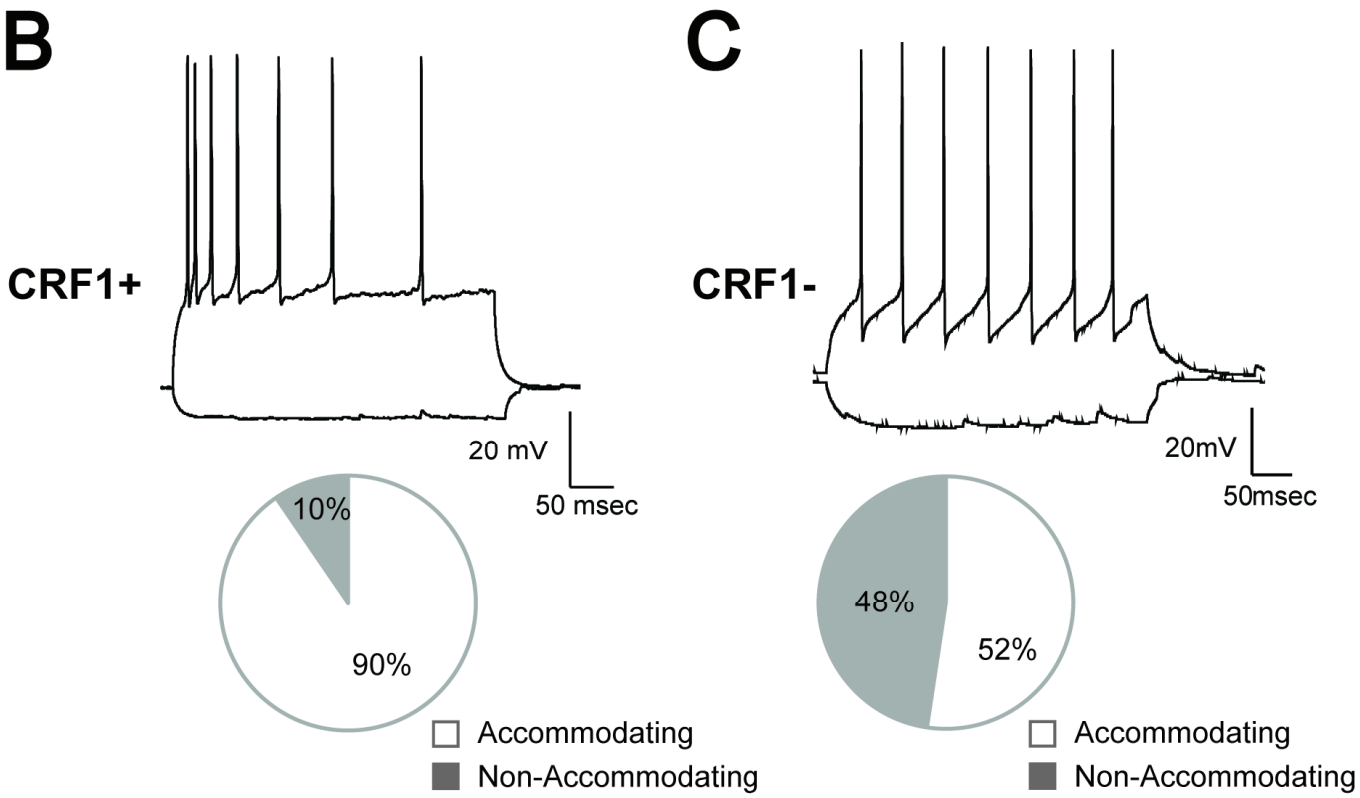

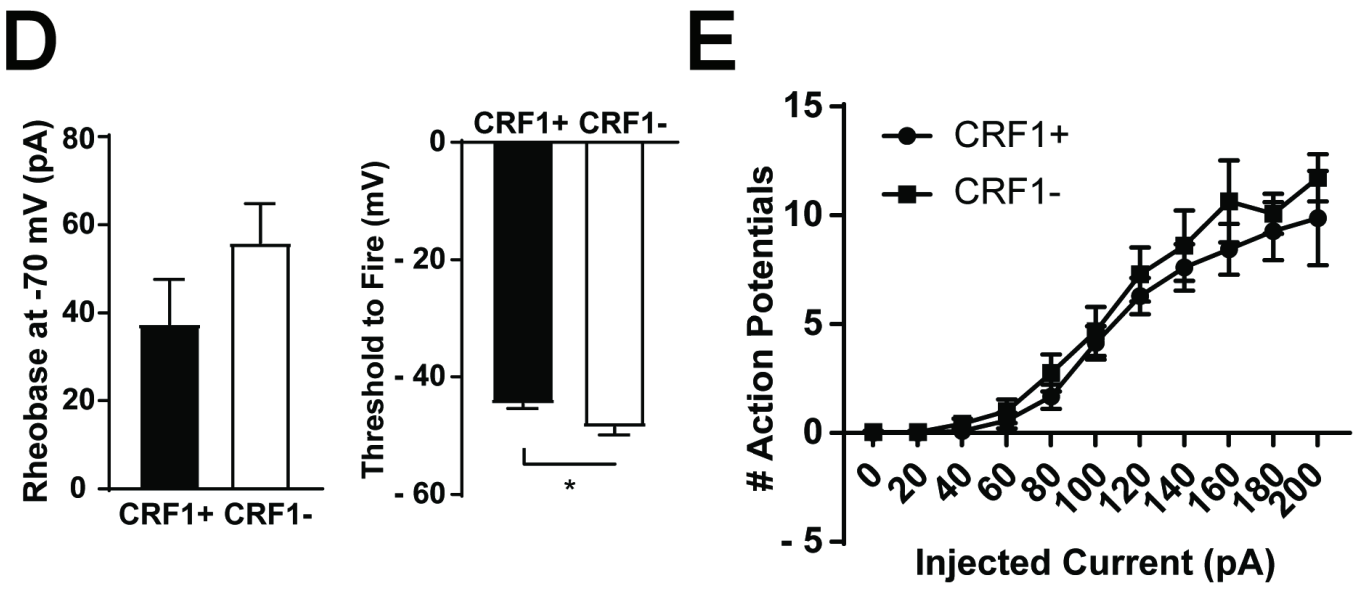

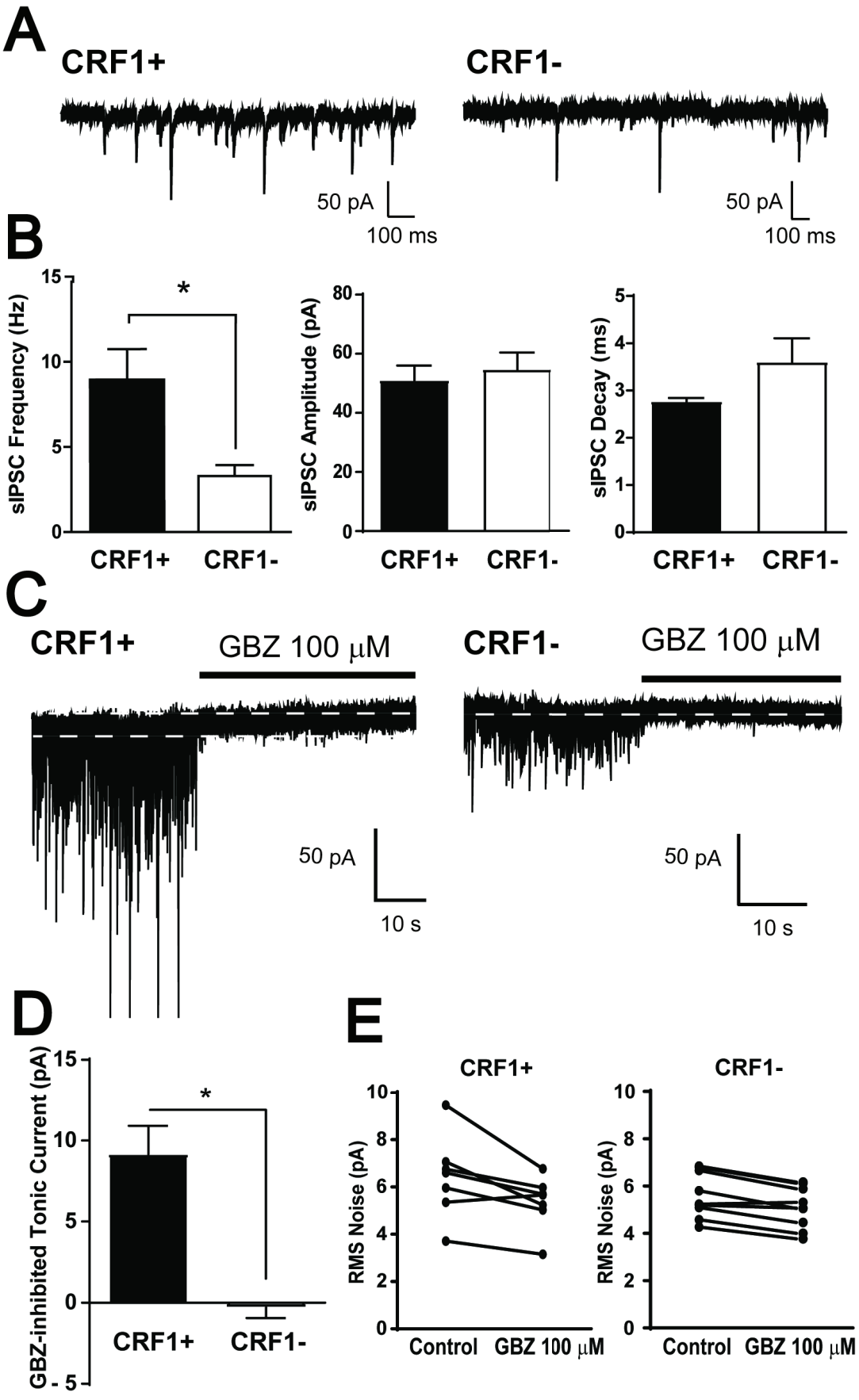

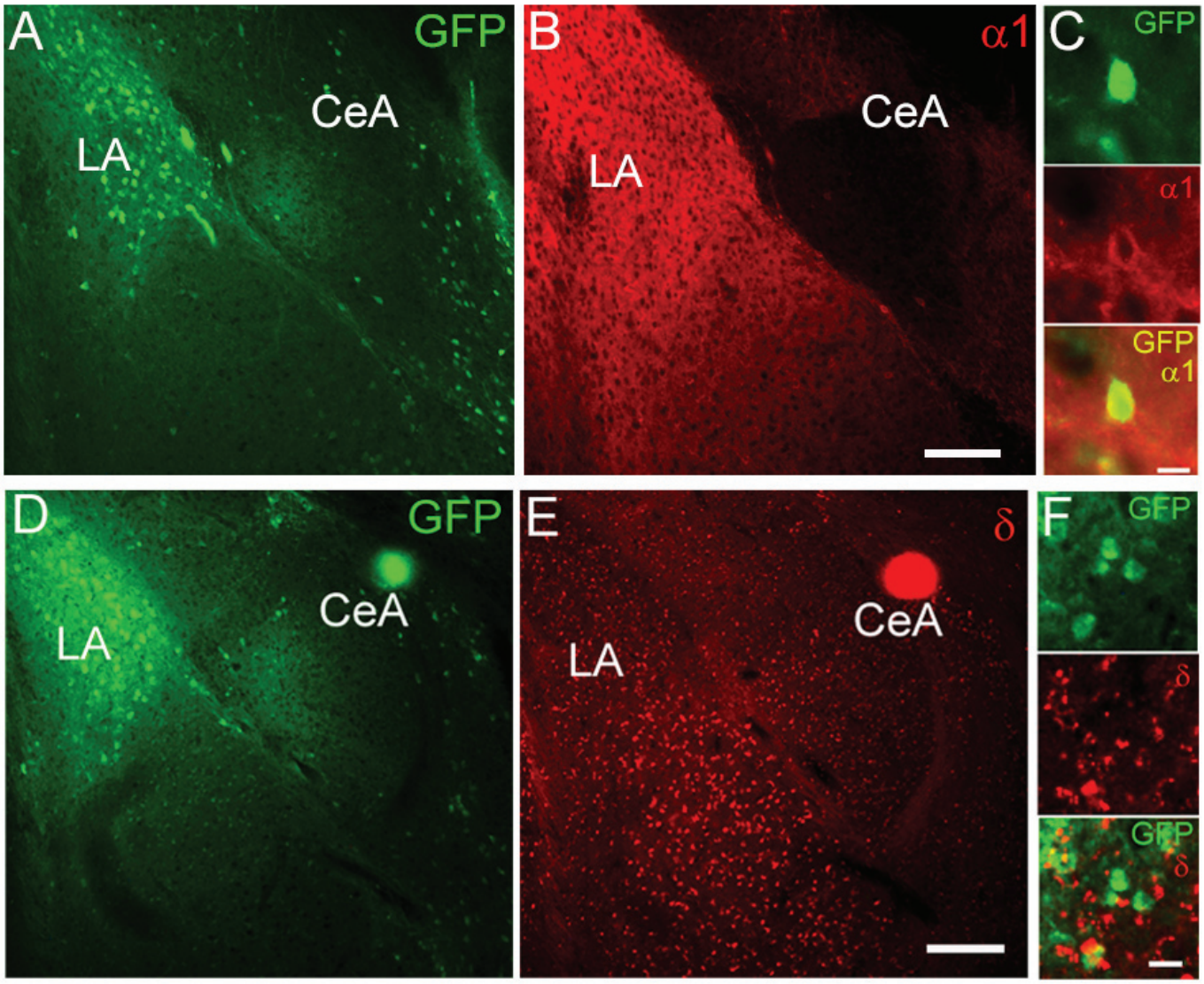

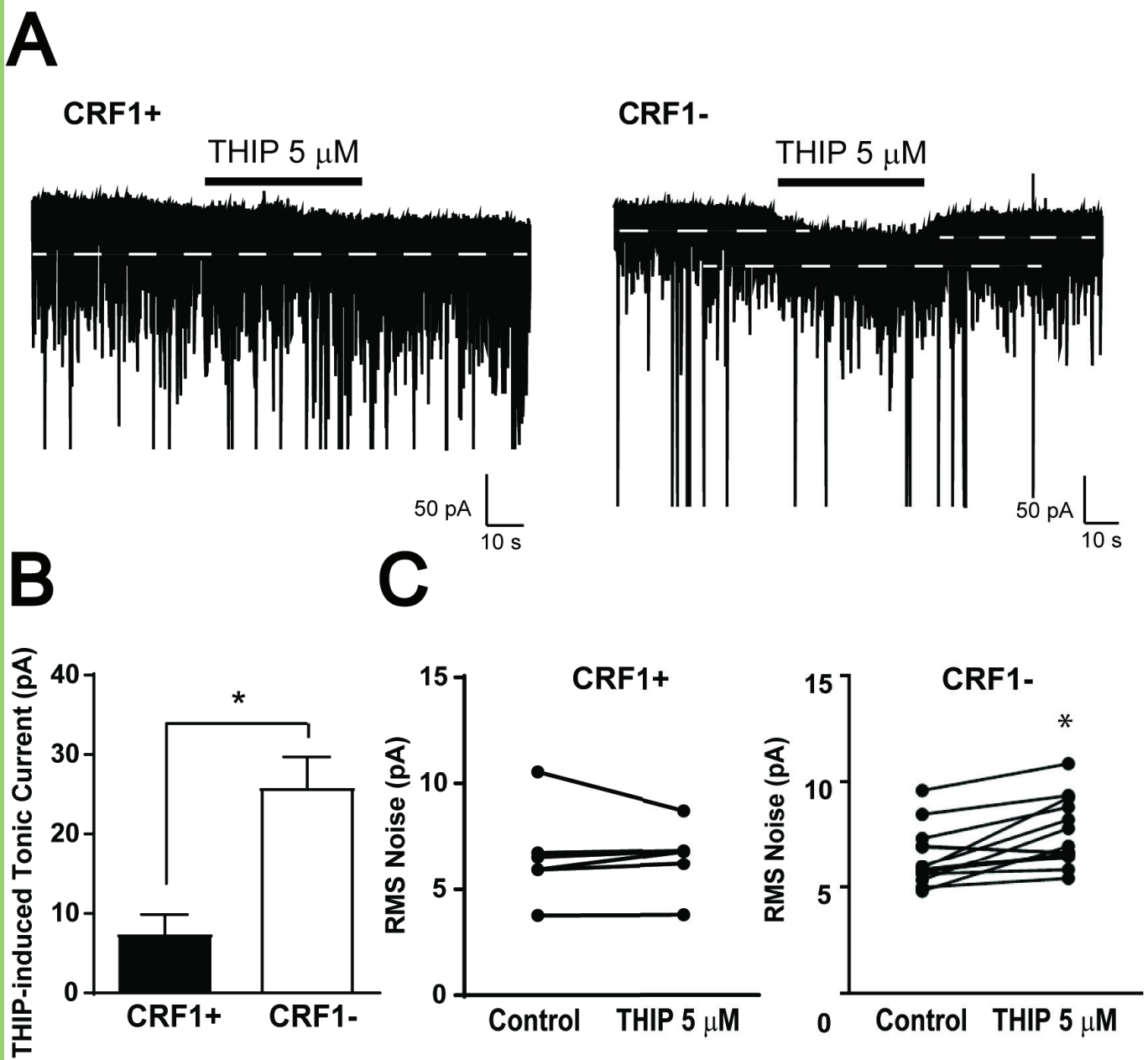

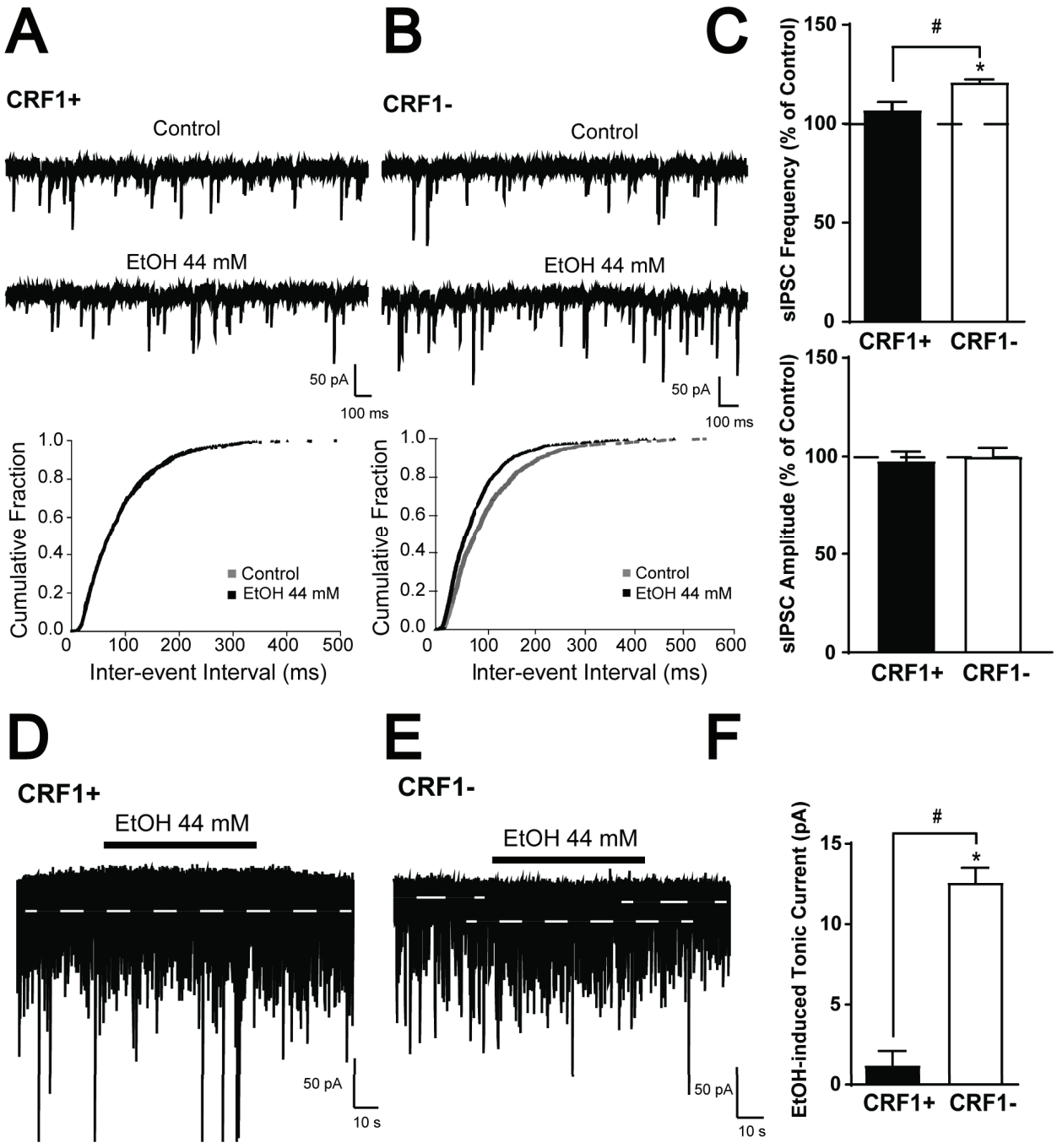

A CRF1+ neurons	Membrane Capacitance Cm (pF)	Membrane Resistance Rm (MΩ)	Decay Time Constant Tau (ms)	Membrane Potential Vm (mV)
AIR (n = 18)	61.4 ± 6.8	153.1 ± 12.1	423.7 ± 63.8	-62.7 ± 2.1
CIE (n = 13)	63.6 ± 6.8	221.1 ± 82.9	430.5 ± 52.4	-61.8 ± 1.6
CIE-WD (n = 10)	66.0 ± 12.2	156.5 ± 21.6	486.0 ± 95.7	-61.9 ± 3.2

B **CRF1+**

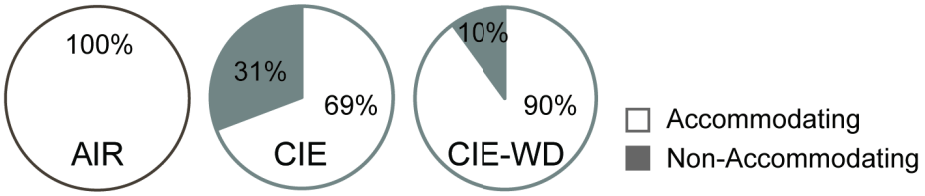

C

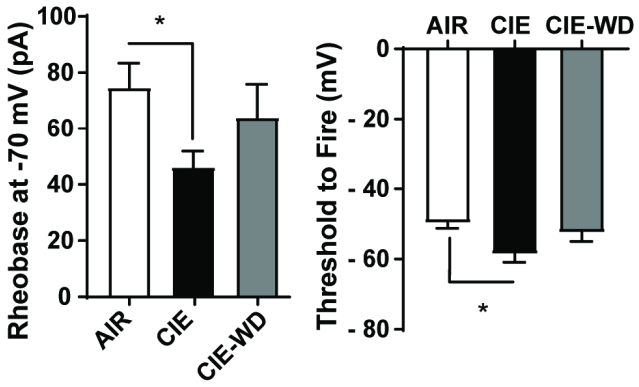

D

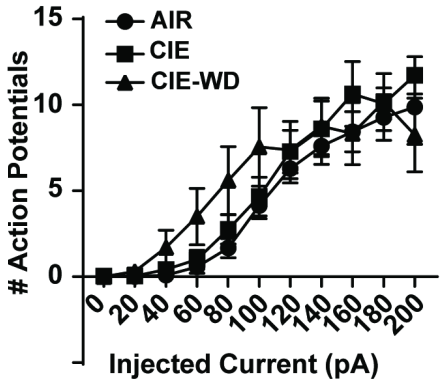

E CRF1- neurons	Membrane Capacitance Cm (pF)	Membrane Resistance Rm (MΩ)	Decay Time Constant Tau (ms)	Membrane Potential Vm (mV)
AIR (n = 10)	74.5 ± 10.3	164.3 ± 30.2	444.6 ± 70.4	-63.7 ± 2.3
CIE (n = 8)	75.0 ± 9.0	119.0 ± 12.2	521.8 ± 87.6	-63.5 ± 3.1
CIE-WD (n = 6)	67.5 ± 15.4	152.0 ± 29.1	631.4 ± 134.5	-65.2 ± 1.5

F **CRF1-**

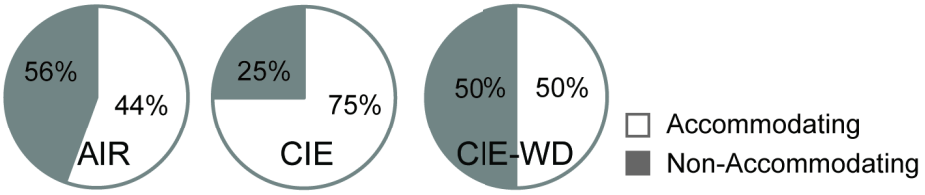

G

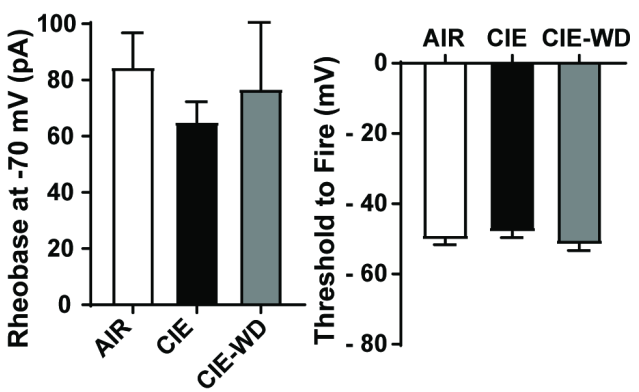

H